A SPATIAL STORY OF DESTRUCTION AND RESTORATION: AL HAWIZEH MARSH, IRAQ

by
Hanin Masboob

A capstone submitted to Johns Hopkins University in conformity with the requirements for the degree of Master of Science in
Environmental Science and Policy

Baltimore, Maryland
May 2021

Abstract

The al Hawizeh Marsh of southern Iraq is one of three marshes belonging to the semi-arid Tigris-Euphrates alluvial salt marsh ecoregion. This extensively freshwater wetland is the only natural marsh remaining in this ecoregion following the intentional environmental degradation imposed by the Saddam Hussein regime by the 1990s. As a result, these once highly biodiverse wetlands became wastelands. With the removal of Saddam Hussein in 2003, Iraqis destroyed the embankments on the rivers, allowing water to flow freely back into the marshes. Thus, this project aimed to evaluate, analyze, and visualize the change the al Hawizeh Marsh due to anthropogenic environmental degradation. Geographic information systems (GIS) was utilized to map and analyze changes in land cover change type, vegetation (NDVI), water (MNDWI), soil moisture (SMMI), soil salinity (SI), and land surface temperatures (LST) from 2000 (pre-flooding) to 2019 (post-flooding). This spatial analysis resulted in overall increases in water, vegetation, soil moisture, soil salinity and LST while the marsh itself yielded decreases in soil moisture, soil salinity, and LST. A random forest statistical analysis was performed to evaluate which variables resulted in the greatest change seen within the al Hawizeh Marsh. Unsurprisingly, water was the most crucial factor responsible for marsh's change from 2000 to 2019. The second and third important change factors included soil moisture content and LST. These results only tell one side of the story; they are not indictive of on ground marsh health. Thus, it is imperative that Iraq implements impactful conservation efforts to promote the restoration and rehabilitation of this critically important and fragile ecosystem.

Keywords: al Hawizeh Marsh, wetland, anthropogenic, degradation, GIS, NDVI, MNDWI, SMMI, SI, LST, random forest

Executive Summary

A career change from a background in medicine and toxicology, the Environmental Science and Policy (ESP) at Johns Hopkins has armed me with the knowledge and technical expertise to make this project a reality. A spur of the moment decision to study the Tigris-Euphrates water basin ignited a passion for the conservation of Iraq's crucial and fragile ecoregion. Projects and papers for numerous ESP and GIS courses—Principles & Methods of Ecology, Open-Source GIS, Web GIS, Environmental Applications of GIS, Global Scarcity in Freshwater Systems, Climate Change on the Front Lines, and Conservation Biology—became the backbone for this capstone. Datasets were readily available from previous GIS courses while ESP courses provided the research and foundation. This capstone utilized several spatial analyses, some familiar and others I employed for the very first time. The statistical analysis portion of this capstone was uncharted territory for me; I came into this project with little-to-no working knowledge of RStudio. However, I can now confidently state that I can employ RStudio and analyze the results for my future research purposes. Specifically, I have grown confident in the Random Forest statical analysis and value its importance in understanding what and how variables impact a study area. Finally, I can confidently state that my scientific writing skills have improved as result of this capstone. The skills, confidence, and admiration gained from capstone have made me a better scientist and is crucial to my future development as I transition from academia and into an inspiring career in environmental conservation and preservation through the lens of climate change in developing nations such as my home country of Iraq.

Table of Contents

List of Tables

List of Figures

List of Images

Introduction

Iraq, with coordinates of 29.5°—37.22°N and 38.45°—48.45°E and covering an area of 438,320 km^2, is known to the world as the *Fertile Crescent*, *Mesopotamia,* and the *Cradle of Civilization* (Salman et al., 2017). Iraq is rich in history, culture, and tradition as it bore witness to the rise and fall of important civilizations of ancient Sumerians, Assyrians, Babylonians, and the Ottomans (Randell, 2003). This inland country possesses a unique geography and climatology, one that is heavily dependent on the downstream flow of the Tigris and Euphrates Rivers—oftentimes referred to as the Twin Rivers—which course through the country from the north to the south (Al-Ansari, 2013; FAO, 2016; Mastrocola, 2017[1]). The Tigris and Euphrates Rivers eventually meet and merge at the city of al Qurnah, forming the Shatt al Arab which continues its southbound downstream flow before draining into the Persian Gulf (Al-Ansari, 2013; FAO, 2016; Mastrocola, 2017[1]). This uniqueness encompasses the country's wetlands—Central Marsh, al Hawizeh and al Hammar Marshes—the largest of its kind in western Eurasia, dubbed as RAMSAR Wetlands of International Important and UNESCO World Heritage Sites (Ramsar, 2015; UNESCO, 2016). Wetlands across the globe act as Earth's "kidneys" by filtering and removing toxins, pollutants and waste from rivers which feed into them (Al-Zaidy et al., 2019).

These wetlands are home to the number of endemic and nearly endemic plant and wildlife and migratory species (Garstecki & Amr, 2011). Given the location of the country and the importance of the services the wetlands provide, it becomes abundantly clear that the Tigris and Euphrates Rivers dictate the livelihoods of every living species in Iraq. One would expect strictly enforced environmental policies which guard the Twin Rivers and the marshes; however, this is not the case. Since the beginning of the 20th Century, Iraq became ground for several domestic and international political conflicts; some of which continuing to this very day (Mastrocola, 2017[1,2,3]). These conflicts, because of anthropogenic and environmental efforts, gave rise to the degradation of the country's natural environment (Mastrocola, 2017[1,2,3]).

The most destructive anthropogenic force came in the form of hydrological damming projects originating from within the country's borders and from those of its neighbors to include Iran, Syria, and Turkey (Dohrmann & Hatem, 2014; Al-Muqdadi, 2019). On Iraqi soil, operating under the guidance of increasing agricultural output, the Hindiya Barrage Dam (established in 1913) on the Euphrates River and the Kut Barrage Dam

***Image 1**: Image 1: Major dams and barrages installed on the Tigris and Euphrates Rivers in Iraq and from its neighbors, Turkey, Syria, and Iran. Marshes are highlighted within the box. Source: Mastrocola, 2017[2].*

(established in 1938) on the Tigris River were constructed (Mastrocola, 2017[2]). The plan was simple: divert the natural flow of the twin rivers away from its course and directly into arable land (Mastrocola, 2017[2]). The consequence of this action directly impacted the country's wetlands access to water by reducing quantity and quality (Mastrocola, 2017[2]). Hailing these barrages as successes, Iraq moved forward, commissioning the Samarra Barrage Dam on the Tigris and the Ramadi Barrage Dam on the Euphrates, for the purpose of creating natural lakes within central Iraq (Mastrocola, 2017[2]). The Haditha Dam on the Euphrates and Mosul Dam on the Tigris became functionally operational by the 1980s (Mastrocola, 2017[2]).

The Saddam Hussein regime is wedged between the construction of the Haditha and Mosul Dams and is solely responsible for laying waste to the wetlands throughout the 1980s and 1990s in a visible demonstration of his political prowess (Al-Ansari & Knutsson, 2011; Mastrocola, 2017[2]). This regime enforced the burning, diverting, draining and installment of various embankments on, around and through the marshes (Al-Ansari & Knutsson, 2011; Mastrocola, 2017[2]). This resulted in habitat fragmentation and loss of landscape connectivity (Richardson & Hussain, 2006). Habitat fragmentation refers to the loss of interconnectivity of a species overall total habitat, often resulting in patches within the environment (Singer, 2016). A consequence of this is a decline in species abundance and environmental decay as mandatory resources become difficult to acquire and support the species fundamental and idealized niches (Singer, 2016; Masboob, 2020). From here, a loss of landscape connectivity was inevitable as native species richness and diversity declined either forcefully through competition with alien/invasive species, hunting and or by migration to another ideal habitat (Masboob, 2020). Satellite imagery of the marshlands captured from the 1980s through the 1990s confirmed this grim reality: the Central Marsh had declined by 97%, al Hammar by 94% and al Hawizeh by two-thirds (SER, n.d.; Al-Ansari & Knutsson, 2011; Mastrocola, 2017[3]). What once were wetlands became wastelands, triggering an early desertification process (Ministry of Foreign Affairs, 2018).

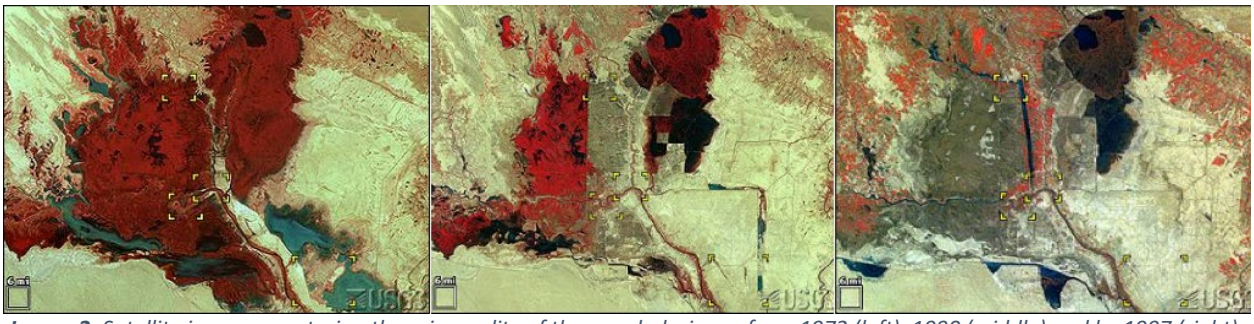

***Image 2**: Satellite imagery capturing the grim reality of the marsh drainage from 1972 (left), 1990 (middle) and by 1997 (right). Source: Mastrocola, 2017[3].*

On the international level, Iraq's neighbors have restricted the flow of the Twin Rivers which promotes the degradation of the wetlands. Singlehandedly, the source of major destruction belongs to Turkey and its Southeastern Anatolia Project or GAP (Dohrmann & Hatem, 2014). Initiated in 1977, Turkey proclaimed that GAP would help push the country into becoming an industrial society to accommodate it rapidly growing population (Dohrmann & Hatem, 2014). GAP, the world's largest hydro-engineering project that swallows 10% of the country's landmass, was set to accomplish this goal by increasing and harnessing

hydroelectricity power from the Tigris Euphrates Rivers (Dohrmann & Hatem, 2014). By its completion year of 2023, GAP would promote the operation of "22 dams, 19 hydroelectric plants, and extensive irrigation systems on the Tigris and Euphrates" (Dohrmann & Hatem, 2014). Consequently, Turkey's original 10% water consumption usage will skyrocket to greater than 50% (Dohrmann & Hatem, 2014). Syria's dependence on hydroelectricity is like that of Turkey's and as a result, have erected their own dams, such as the Tabqa Dam, to control the flow of the Euphrates River (Dohrmann & Hatem, 2014; Richardson, 2018). Such projects have led to alarming consequences in Iraq: in 2018, with the operation of Turkey's controversial Ilisu Dam, the Tigris' volume decreased so drastically that Baghdadis were able to wade through the river, moving from one side of the riverbed to the other with disturbing ease (Ellis, 2019). Another source of major destruction was triggered by the U.S.-led invasion in 2003 and the birth of the militant group ISIS/ISIL/Daesh (Al-Azzawi, 2016; CRF, 2019; Ellis, 2019). The U.S. paralyzed and suffocated Iraq with continuous intensive bombing combined with thousands of heavy military tanks, artilleries and vehicles cruising between some 503 American and coalition military bases (Al-Azzawi, 2016).

The U.S. Army, Air Force and Navy's aggressive movements initiated an early and intense desertification process across the country as it literally forced a change in the country's internal soil structure and texture by triggering soil loss, top-soil loss of organic nutrients, and soil erosion (Al-Azzawi, 2016). Fertile soils became a layer of ceramic, and these can affect the country's food security (Fitzpatrick, 2004; Al-Azzawi, 2016). Furthermore, the country became victim to frequent and prolonged sand and dust storms due to this desertification process, promoted by the soil erosion, changes to the soil and lack of vegetation (Al-Azzawi, 2016). Daesh's emergence further exacerbated the country's instability and continued environmental degradation: the U.S. forces polluted Iraq's water, soil, and air while Daesh took the Twin Rivers hostage (Al-Azzawi, 2016; Ellis, 2019). Daesh seized control of the Ramadi Barrage, shutting off the Euphrates' flow, hammering the last nail of the wetland's coffin (Al-Azzawi, 2016). As a show of their prowess, Daesh took it upon themselves to destroy several oil and gas fields, purposely spilling and contaminating the environment with hazardous waste (Al-Azzawi, 2016). The perfect anthropogenic destructive cocktail, one that has been in the works from the 20th Century and carries on today, has been served.

Iraq is no stranger to the impacts of climate change — in the simplest of terms, the country is bearing witness to increased temperatures, decreased precipitation, increased evaporation, increased water salinization and increased prevalence of drought and sand and dust storms (Ministry of Foreign Affairs, 2018). Water scarcity is Iraq's most prominent and on-going issue as only 8% of the Iraq's water comes from within the country while 71% is drawn from Turkey, 6.9% from Iran and 4% from Syria (Ministry of Foreign Affairs, 2018). Due to its location, Iraq is subjected to the Sharqi and Shamal winds, both of which blanket the country with dry winds (Ministry of Foreign Affairs, 2018). In combination with increased temperatures and evaporations, these dry winds further promote the desertification process by allowing dry air to suffocate the country resulting in the sand and dust storms (Ministry of Foreign Affairs, 2018). It was reported that between 1951 to the 1990s, Iraq experienced an annual of 24 days per year of sand and dust storms (SDS); however, by 2013, these incidences have increased to 300 annually (Ministry of Foreign Affairs, 2018). The degradation of the wetlands, land, soil has only been fueled by the decline in precipitation, in response to increases in temperatures and

evaporation, leading to occurrences natural disasters (Ministry of Foreign Affairs, 2018). These environmental impacts, working together with anthropogenic factors, paved way for reducing the country's biodiversity, leading to extinctions in severe cases (SER, n.d.).

A silver lining can be drawn from these events; in 2003, empowered by removal of Saddam Hussein, locals took it upon themselves to destroy nearly all embankments on the Tigris and Euphrates, allowing the waters to flood the marshes once more (Aoki et al., 2011; Douabul et al., 2012; Mastrocola, 2017[3]). These efforts have brought some much-needed good news: the marshes were slowly beginning to reclaim their extents, vegetation was regrowing, and wildlife was making a comeback (Aoki et al., 2011; Garstecki & Amr, 2011; Douabul et al., 2012). However, conservationists are painting an unfortunate image: the haphazard reflooding efforts may have caused more degradation in the wetlands rather than improvements (Douabul et al., 2012). The Garden of Eden's future is plagued with uncertainty in the face of economic, environmental, political and security uncertainty.

Thus, the purpose of this project is to evaluate, compare, and visualize the extent of environmental degradation to the al Hawizeh Marsh following its deliberate drainage and then it's reflooding efforts. Specifically, this project will employ spatial analysis, through GIS and remote sensing, to understand the environmental consequences this wetland had undergone due to the Saddam Hussein regime. Here, draining is referred to as pre-flooding and defined as the degraded status of the wetland by the end of the 1990s while post-flooding refers to the status of the wetlands following the destruction of embankments, dikes, and canals in 2003. For this analysis, pre-flooding is defined as the year 2000 while post-flooding is defined as the year 2019. It is hypothesized that the al Hawizeh Marsh will have increased its extent resulting in an increase in vegetation, water, soil moisture content, soil salinity, and surface temperatures from 2000 to 2019.

Study Area

With coordinates of 31.34' 37" N and 47.41' 05" E, the Iraqi marshes ("Ahwar") are both the world's and the Middle East's and Western Eurasia largest freshwater water ecosystem (SER, n.d.). These alluvial salt marshes include the Central Marsh (southeast of Baghdad), al Hammar Marsh (south of Euphrates and east-southeast of Nasiriya) and the al Hawizeh Marsh (east of Tigris and southeast of Amara), once covering an area of 15,000 km^2 to 20,000 km^2 (Aqrawi et al., 2006; Aoki et al., 2011; Al-Ansari & Knutsson, 2011). The wetlands lay within the Lower Mesopotamian Plain on the Stable Self (Aqrawi et al., 2006). The Lower Mesopotamian Plain is a low, flat, and broad area, dominated by shallow lakes (fresh and brackish waters) and dense vegetation or marshes (Aqrawi et al., 2006). The low, flat, and broad nature of this region makes it prone to major floods, particularly following spring melt (Aqrawi et al., 2006). Surface sediments of these wetlands are comprised of silt (50-60%), sand (20-27%), and clay (17-22%) and appear black, gray, or olive green in color (Richardson, 2018; Aqrawi et al., 2006).

The al Hawizeh Marsh (Haur al Hawizeh) is the study area of this project and is located at 31° 25' 29'' North latitude and 47° 38' 44'' East longitude, in the Maysan (Misan or Missan) and Basrah (Basra) governorates (Al-Ansari & Knutsson, 2011; Rubec & Young, 2014). This marsh possesses an altitude range of 4 to 11 meters above sea level (RSIS, 2012[1]; Nature Iraq, 2017). The total area of al Hawizeh Marsh has been reported between 137,700 hectares (1,377 sq. km) to 164,023 hectares (1640.23 sq. km) depending on the source of reference (RSIS,

2012[1]; Nature Iraq, 2017). What makes this wetland so unique compared to its counterparts of the Central and al Hammar Marshes is that extensively a freshwater marsh even though it belongs to the Tigris-Euphrates alluvial salt marshes ecoregion (RSIS, 2012[1]). Furthermore, it is the only marsh that is vastly permanent and seasonal, dominated by fresh and brackish waters (RSIS, 2012[1]). These fascinating characteristics of the al Hawizeh Marsh promote the size of this wetland, the only one found in all Western Eurasia (RSIS, 2012[1]). The al Hawizeh Marsh is also a transboundary marsh; 70-80% of its total area is found in Iraq and the remaining 20-30% belong to Iran (Rubec & Young, 2014; Nature Iraq, 2017). As such, this marsh is supplied by the Tigris' two distributaries, Al-Musharah and Al-Kahla'a, and the Karkheh River from Iran (Al-Ansari, 2013; Rubec & Young, 2014; FAO, 2016; Mastrocola, 2017[1]; Nature Iraq, 2017).

Formed some 3,000 years ago, these interconnected systems of marshes are under the influence of Iraq's semi-arid or steppe climate (Al-Ansari, 2013; Ministry of Foreign Affairs, 2018; UNESCO, n.d.). Precipitation in this climate zone is mild, with annual rainfall ranging from 200 mm to 400 throughout the spring and winter months (Ministry of Foreign Affairs, 2018). As a semi-arid zone, temperatures can skyrocket to a blistering 46°C in the summer and drop down to 5°C in the winter (Ministry of Foreign Affairs, 2018). The most important hydrological feature for these alluvial salt marshes includes the Tigris and Euphrates Rivers which flow downstream from Turkey and Syria (Mastrocola, 2017[1]). After passing through the marshes, the Tigris and Euphrates meet and merge at the city of al Qurnah to form the Shatt al-Arab ("the Arab's River"), which continues to flow for 190 km downstream before draining into the Persian Gulf (Al-Ansari, 2013; FAO, 2016; Mastrocola, 2017[1]).

This ecosystem sits in a semi-arid climate yet is home to a number of endemic, semi-endemic and migratory species (Garstecki & Amr, 2011). The Iraqi marshes are relatively young compared to other wetlands; so young in fact, there is evidence of ongoing vertebrate evolutionarily processes resulting in several endemic species and subspecies (Garstecki & Amr, 2011). Migratory species, such as birds, use these marshes as their nesting, nursing, feeding and resting grounds (Garstecki & Amr, 2011). Fish, swimming from the Persian Gulf, utilize these marshes as their spawning grounds (Garstecki & Amr, 2011). Several endangered and threatened species call these wetlands their home, including the pygmy cormorant (*Phalocrocorax pygmeus*), white-tailed eagle (*Haliaeetus albicilla*), Euphrates Soft-shelled Turtle (*Rafetus euphraticus*) and the Smooth-coated Otter (Lutrogale perspicillata maxwelli) (Garstecki & Amr, 2011). Vegetation in the marshes both aquatic and semi-aquatic and is dominated by reed (*Phragmites australis*) (Garstecki & Amr, 2011).

An ecological assessment was performed between 2003 and 2005 to assess the restoration process of the wetlands following uncoordinated flooding efforts (Richardson & Hussain, 2006). Results from this assessment and other analyses detailed a grave picture: salinity had increased in the wetlands, soil, once fertile, had transformed into a layer of ceramic with detection of heavy metals and an imbalance of major constituents in water bodies (Fitzpatrick, 2004; Richardson & Hussain, 2006; Hassan et al., 2010; AlMaarofi et al., 2014; Talib, 2017). Changes had occurred in the marshes' biodiversity at varying trophic levels: vegetation was increasing in abundance, but alien and invasive species were overtaking native flora while the diversity (i.e., species richness) and abundance of primary producers has not yet recovered meaning that productivity of the marshes remains to be seen (Hamdan et al., 2010; Ameen et al., 2019). Zooplankton, a primary consumer which feeds on phytoplankton, showed mixed

results in species richness and fitness (Salman et al., 2014; Ameen et al., 2019). Fish stocks, which is an important source of income, varied across the marshes and was dominated by invasive and alien species (Hussain et al., 2013; Mohamed et al., 2017; Al-Thahaibawi et al., 2019). Two key factors must be stated: first, results varied across the marshes; the al Hawizeh Marsh is the only "natural" remaining wetland and proved to maintain some of its pre-degradation characteristics (Al-Thahaibawi et al., 2019). Of course, this is not true to the marsh in its entirety; the above statement rings true for the unaltered regions of the marsh which is explicit to its northeastern reaches compared to its south and southeastern extent (Hassan et al., 2010; Al-Thahaibawi et al., 2019; Ameen et al., 2019). Second, a notable increase in species diversity does not equate to a successful marsh restoration (Al-Thahaibawi et al., 2019; Masboob, 2020). The abundance of alien species across the wetland's points to an unhealthy ecosystem as these new species—flora or fauna—outcompete native species for resources simply because they are better adapted or tolerant to the marsh's new abiotic changes (Masboob, 2020).

Climate change has impacted the wetland's restoration process in a series of natural hazards such as droughts, floods, and dust and sandstorms (World Bank Group, n.d.). Flooding results from spring melt which increases the annual discharge of the Twin Rivers; the Tigris' discharge increases from February through June while the Euphrates sees an increase between March through July (World Bank Group, n.d.). As a result of this burst in volume, downstream flow roars through the country, flooding the marshes and southern extents particularly (World Bank Group, n.d.). While floods result in increased water volume, the quality of the water pouring into the wetlands will vary in salinity, nutrients, metals, toxins, waste, and other pollutants which can result in harmful blooms (Hasab et al., 2020). The frequency and intensity of droughts and sand and dust storms are a result of decreased precipitation, increased temperatures, increased evapotranspiration, low vegetation density, and low soil moisture (World Bank Group, n.d.; UNEP et al., 2016; Hameed et al., 2018; Ministry of Foreign Affairs, 2018; Albarakat & Lakshmi, 2019; Al Ameri et al., 2019). This is primarily due to upstreaming damming projects and the destruction of the marshes in the 80s and 90s (World Bank Group, n.d.; Hameed et al., 2018; Ministry of Foreign Affairs, 2018; Al Ameri et al., 2019).

Rainfall, in the southeast, has decreased by 0.88 mm per month per century while temperatures have increased, across the country, by 0.7°C per century (Ministry of Foreign Affairs, 2018). The rate of evapotranspiration, coupled with increasing temperatures and decreasing precipitation, consequently led to an alarming drying the country's soil, effectively depleting groundwater levels of the Tigris-Euphrates Rivers basin (Ministry of Foreign Affairs, 2018). Some studies have suggested that by 2040, the Tigris and Euphrates will be completely dry in Iraq (Ministry of Foreign Affairs, 2018). This, of course, does not consider the impact of water flow manipulation, changes in the river's hydro-period and hydro-patterns, from the marshes due to gain access to oil reservoirs beneath these critical ecosystems (Ministry of Foreign Affairs, 2018; Richardson & Hussain, 2006; Richardson, 2018). Climate change, along with human activity, are turning these wetlands into drylands.

Methods

The methodology for this project is divided into two main parts. The first involved the utilization of GIS software to include both ArcGIS Pro and QGIS. GIS software was used to perform

topographical and land cover analyses to determine the extent of environment change across the al Hawizeh Marsh in 2000 and again in 2019. The second part of the methodology is running a statistical analysis, in the RStudio software to determine which variables imposed the greatest changes to the al Hawizeh Marsh.

Data Acquisition

Landsat data of the al Hawizeh was downloaded from the USGS Earth Explorer website. This included the Landsat 5 (L5) for the year 2000 and Landsat 8 (L8) for the year 2019 spatial images. Both these Landsat images were selected with similar Worldwide Reference System (WRS) Path and Row to ensure scene similarities. For this project, the WRS Path is 166 and the WRS Row is 38. The L5 image was acquired May 21st, 2000, and the L8 was acquired on May 26th, 2019. For both images, the following search criteria was imposed: Land Cloud Cover was less than 10%, Scene Cloud Cover was less 10% and possessed a Tier 1 Collection Category. Finally, these two images also reflected non-drought years for more adequate comparisons. Similarly, Digital Elevation Model (DEM) was downloaded from the Earth Explorer website. This geotiff shapefile possessed a resolution of 1-ARC second, and an acquisition date of February 11th, 2000. The Iraqi Boundary and Protected Areas shapefiles were obtained from the following databases: DIVA-GIS (Iraq boundary), and Protected Planet (protected marsh extent).

Data Processing

From the acquired DEM, a Slope layer was produced utilizing the Raster Analysis geotools in QGIS. The Landsat 5 and 8 rasters were processed within the Semi-Automatic Classification Plugin (SCP) in QGIS. In the Band set tab, only the spectral reflectance value bands were added as Band Set 1 and Band Set 2 to clip these rasters to the same extent. Band Set 1 included bands bands 1, 2, 3, 4, 5, and 7 for Landsat 5 TM and Band Set 2 included bands 2, 3, 4, 5, 6, and 7 for Landsat 8 OLI. In the Preprocessing tab, the band sets were clipped using the Clip Multiple Rasters tool in SCP using the following extent ranges: upper left 670396.00 and 3436245.00 and lower right 837135.00 and 3530205.00 meters for L8. The extent for L5 was upper left 670455.00 and 3444255.00 and lower right 836145.00 and 3529995.00 meters. This was the closest extent created for both images as the Landsat 5 was generally smaller compared to the Landsat 8 image. These new clipped files, identified as L8 Clip and L5 Clip, were saved in the geotiff format, and utilized in the variable analysis as described below. All the newly created rasters were reprojected in QGIS to the WGS 84/UTM zone 38N coordinate reference system, the coordinate system of the wetland shapefile obtained from Protected Planet.

Variable Analysis

When attempting to evaluate the degradation impacts on wetlands, the most important factors are vegetation, water, and soil (Lv et al., 2019). As such, these factors will be utilized to examine the anthropogenic impacts of the Saddam Hussein regime on the al Hawizeh Marsh following their draining (Landsat 5 or L5) and reflooding (Landsat 8 or L8) efforts.

Normalized Difference Vegetation Index (NDVI)

To assess the health of the vegetation following reflooding events, an NDVI analysis was

performed on the al Hawizeh Marsh. NDVI describes the relative health and density of vegetation (USGS, n.d.[1]). To run this analysis, the following formula was used:

$$\boldsymbol{NDVI} = \frac{Near\ Infrared\ (NIR) - Red\ Band\ (R)}{Near\ Infrared\ (NIR) + Red\ Band\ (R)}$$

Therefore, for L5, the equation reads: Band 4 -/+ Band 3 and for L8, it reads: Band 5 -/+ Band 4 (USGS, n.d.[2]). The final layers are identified as NVDI_L5 and NDVI_L8.

Modified Normalized Difference Water Index (MNDWI)

To assess the health of wetland's water, the MNDWI was utilized rather than the standard NDWI. The modified version was chosen because it eliminates all non-water and coastline features such as built-up land, soil, and vegetation by removing them or rendering them as negative values (Xu, 2006). This allows users to focus on the water bodies completely free from distractions (Xu, 2006). The MNDWI's formula is as follows:

$$\boldsymbol{MNDWI} = \frac{Green\ (G)\ -\ MIR\ (Short - wave\ Infrared)}{Green\ (G)\ +\ MIR\ (Short - wave\ Infrared)}$$

Therefore, for L5, the equation reads Band 2 -/+ Band 5 and for L8, it reads: Band 3 -/+ Band 6 (USGS, n.d.[2]). The final layers are identified as MNDWI_L5 and MNDWI_L8.

Soil Moisture Monitoring Index (SMMI)

To assess the health of the marshes' soil, the SMMI was employed as it can quantify the moisture content of the bare soil at depths 0 to 5 cm (Lv et al., 2019). The SMMI's formula is as follows:

$$\boldsymbol{SMMI} = \frac{\sqrt{NIR\ (Near\ Infrared) + SWIR\ (Short{-}wave\ Infrared)}}{\sqrt{2}}$$

Therefore, for L5 the equation reads the square root of Band 4 + Band 7 and for L8, it reads: the square root of Band 5 + Band 6 (USGS, n.d.[2]). The final layers are identified as SMMI_L5 and SMMI_L8.

Salinity

To understand the impact of water quality on the al Hawizeh Marsh, soil salinity was assessed. Soil salinity is a key parameter in understanding the quality of the marsh's water as salinization can be the result of vegetation clearance, intensive agriculture, and or altered freshwater discharge (Herbert et al., 2015; Hasab et al., 2020). Hasab et al. (2020), note that the Tigris' and Euphrates' discharge zones into the Iraqi Marshes ranges from 0.5 to 2 ppt. The equation, as shown below, depends on the vegetation's growing conditions which helps to spatially map the soil salinity distribution (Elhag, 2016).

$$\boldsymbol{SI} = \frac{Red \times Near\ Infrared}{Green}$$

Therefore, this equation reads Bands 3 times 4 divided by 2 for L5 and Bands 4 times 5 divided 3 for L8. The final layers are identified as SI_L5 and SI_L8.

Temperature

Iraq's temperature data is either incomplete or dated. As such, the land surface temperatures of the al Hawizeh were manually calculated from the Landsat 5 thermal Band 6 and the Landsat 8 thermal Band 10 based on the *GIS & RS Solution* (2020[1,2]) tutorials. These were chosen to represent average conditions during these two years. These steps were performed in QGIS and utilized the Raster Calculator following specified calculations (GIS & RS Solution, 2020[1,2]). These calculations can be found in the Appendix A. Once these steps were completed, the final layers, LST_L5 and LST_L8, are appropriately symbolized and overlaid on the al Hawizeh Marsh's extent.

Supervised Classification

A supervised classification was performed to establish major land cover classes within the marsh from the Landsat 5 and Landsat 8 spatial images. This was accomplished using the Semi-Automatic Classification Plugin (SCP) in QGIS. Regions of Interest (ROIs) were manually drawn on the Landsat images and designated a specific class: Water, Marsh, Land for L5 and L8. For L5, an additional class, Drained Water, was created to emphasize the draining of the al Hawizeh Marsh. Once the ROIs were completed for both images, the most visually accurate land cover classification result was obtained using the Macro Class ID of the 4 aforementioned classes using the Spectral Angle Mapping algorithm. This resulted in the L8_Super and L5_Super layers.

Land Cover Change

A stratified sampling design and classification error matrix was created for both Landsat images using the SCP tool. Land cover change was assessed from the pixel count in Raster Analysis geotool and the Postprocessing (Land cover change) tool within SCP. Errors of Omission, Errors of Commission, Producer's Accuracy and Overall Accuracy were manually calculated to analyze the results of the produced thematic change layers for the L5 and L8 spatial images. Once this was completed, a change cover detection analysis, emphasizing spectral distance, was performed. This produced two rasters: the spectral angle distance raster and the spectral distance change raster. The spectral angel distance raster calculated the spectral angle for each corresponding pixel between Landsat 5 to Landsat 8's supervised classifications while the spectral distance change raster visualized the corresponding pixels, which possessed a spectral angle greater than 10°. The result was the change in land cover from 2000 to 2019. This layer was identified as SpectralDistanceBandSets_1_2 and later shortened to SpectraDi.

Statistical Analysis: Random Forest

In order to identify which factor(s) posed the greatest impacts on the marshlands, a Random Forest (RF) approach was utilized. Per Harris and Taylor (2015), "*RF works by building a large number of classification and regression trees and aggregating the results. For each regression*

tree, a bootstrap sample is drawn from the dataset, and the tree is built by selecting from a random sample of the predictors at each node." In essence, Random Forest will determine which biophysical predictors are most important in determining marshland health. The random forest classification method does this by ranking the order of importance of the variables via averaging thousands of bootstrapped regression trees. The bootstrapped trees are randomly generated by using a random subset of the predictor variables from the water (MNDWI) index, soil moisture (SMMI), salinity (SI), land surface temperatures (LST), and land cover change (Supervised Classification) Landsat 5 and Landsat 8 data points.

To run the random forest, data points from a stratified random sample, in QGIS, were created. Prior to this event, however, a fishnet was generated for Landsat 5 as this raster possessed an overall smaller extent in comparison to the Landsat 8 raster. The Create Fishnet geotool was utilized in ArcGIS Pro using the Landsat 8 spatial extent, to generate points in areas that otherwise were "cut off" due to extent size differences. Once this was accomplished, the shapefile was imported to QGIS to run the stratified random points.

First, Regular Points were created with the following the parameters: 200 meters point spacing/count and 200 meters initial inset from corner to reduce potential spatial autocorrelation influencing the results. Then, utilizing the Point Sampling tool, a geopackage (.gpkg) was created in QGIS from the Regular Points sampling points to draw values from the following layers: SpectraDi, LST_5 and LST_L8, L5_Super and L8_Super, MNDWI_L5 and MNDWI_L8, SMMI_L5 and SMMI_L8 and SI_L5 and SI_L8 and the fishnet layer. Next, a random selection of 100 points was run and exported as a comma-separated value (.csv) file. In Excel, these values were cleaned up to remove any empty fields generated from the random point selection. A final csv file was created with a total of 500 points which were utilized in the random forest analysis in R (version 4.0.5) to run 4,000 trees. It should be noted that the csv file contained categorical variables (L8_Super, L5_Super, and SpectraDi) which needed to be converted into factors prior to running the model.

In the model, the variable SpectraDi reflected the change and no change in the al Hawizeh Marsh. Thus, the model assessed which variables—LST, MNDWI, SI, and SMMI—influenced whether change or no change in the marsh land cover occurred at between 2000 and 2019. This resulted in the Mean Decrease Accuracy and the Mean Decrease Gini. The Mean Decrease Accuracy plot determines how accurate the model is after it excludes each variable or how important that variable is in the overall model accuracy (Martinez-Taboada & Redondo, 2020). The most important variables are plotted at the top while the least important variables are plotted at the bottom (Martinez-Taboada & Redondo, 2020). The higher the variable is on the Mean Decrease Gini, the more important it is for the results (Martinez-Taboada & Redondo, 2020). Variable importance plots were created to determine and rank the variables that greatly impacted the marsh based off the Mean Decrease Accuracy results. Finally, Partial Dependence Plots (PDP) were produced, for both change and no change categories to assess which biophysical variables were most important in determining land cover change.

Results

The results section is split into two primary sections. The first section details the results obtained from variable analysis which includes DEM and Slope, the Supervised Classification, NDVI and MNDWI, SI and SMMI and finally, LST for Landsat 5 and Landsat 8. The second section details the results obtained from the Random Forest statistical analysis. The appropriate graphics (figures, tables, and plots) follow the discussed analysis.

Variable Analysis

DEM & Slope

Elevation and slope, in **Figure 1**, depict the low-laying and flat characteristics typical of a wetland.

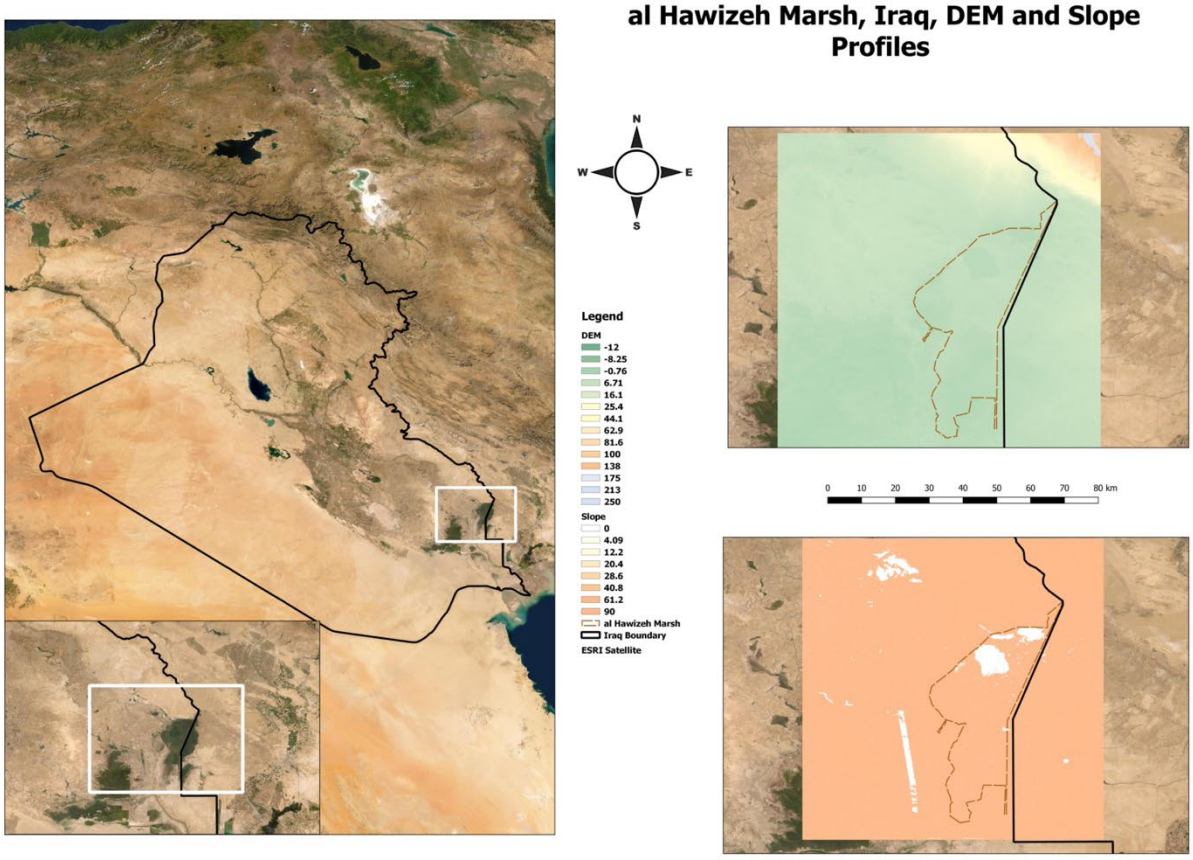

***Figure 1**: DEM and slope analysis results of the al Hawizeh Marsh.*

Supervised Classification & Land Cover Change

The results from the supervised classification (**Figure 2**) verify the wetland drainage story by the end of the 1990s. In the Landsat 5 classification, four major classes were identified, for simplification: water, marsh (i.e., vegetation), land (i.e., urban, and rural) and drained marsh. The results obtained highlight the extent of the drainage (top left map, in yellow) the Saddam Hussein administration imposed on this fragile yet crucially important ecosystem. Based on the pixel count of the land cover change, by 2019, the wetland had regained water and marsh vegetation by 722,432 and 538,389 acres respectively (bottom left map). **Tables 4** and **5**, in

Appendix B, assess the land cover change based on supervised classifications from the pixel count.

***Table 1**: Landsat 5 Classification Error Matrix to evaluate the validity of the supervised classification analysis.*

Landsat 5 Classification Error Matrix

	Water (1)	**Marsh (2)**	**Land (3)**	**Drained Marsh (4)**
Errors of Omission	6/8*100 = **75%**	5/10*100 = **50%**	10/13*100 = **76.92%**	2/9*100 = **22.22%**
Errors of Commission	8/10*100 = **80%**	5/10*100 = **50%**	7/10*100 = **70%**	3/10*100 = **30%**
Producer's Accuracy	2/8*100 = **25%**	5/10*100 = **50%**	3/13*100 = **23.08%**	7/9*100 = **77.78%**
User's Accuracy	2/10*100 = **20%**	5/10*100 = **50%**	3/10*100 = **30%**	7/10*100 = **70%**
Overall Accuracy	17/40*100 = **42.5%**			
Overall Error	100 – 42.5 = **57.5%**			

***Table 2**: Landsat 8 Classification Error Matrix to evaluate the validity of the supervised classification analysis.*

Landsat 8 Classification Error Matrix

	Water (1)	**Marsh (2)**	**Land (3)**
Errors of Omission	0/1*100 = **0%**	3/9*100 = **33.33%**	12/20*100 = **60%**
Errors of Commission	9/10*100 = **90%**	4/10*100 = **40%**	2/10*100 = **20%**
Producer's Accuracy	1/1*100 = **100%**	6/9*100 = **66.67%**	8/20*100 = **40%**
User's Accuracy	1/10*100 = **10%**	6/10*100 = **60%**	8/10*100 = **80%**
Overall Accuracy	15/30*100 = **50%**		
Overall Error	100 – 50 = **50%**		

From these two supervised classifications, a land cover change assessment shows land cover class changes throughout the wetland. The report, which details the land cover class changes, utilizing L5_Super as the reference classification and L8_Super as the new classification, can be found in **Appendix C, Image 3.** By far, the largest change is due to Landsat 8's water, marsh, and land classes reclaiming the drained marsh class of Landsat 5. These are labeled 10, 11, and 12 in the legend below (**Figure 2**). Other notable class changes include the water to marsh (2), water to land (3), marsh to water (4), marsh to land (6), land to water (7), and land to marsh (8). In other words, by 2019, there is an overall increase in the wetland's water and marsh vegetation while also reclaiming the once drained wetland for urban and rural occupation.

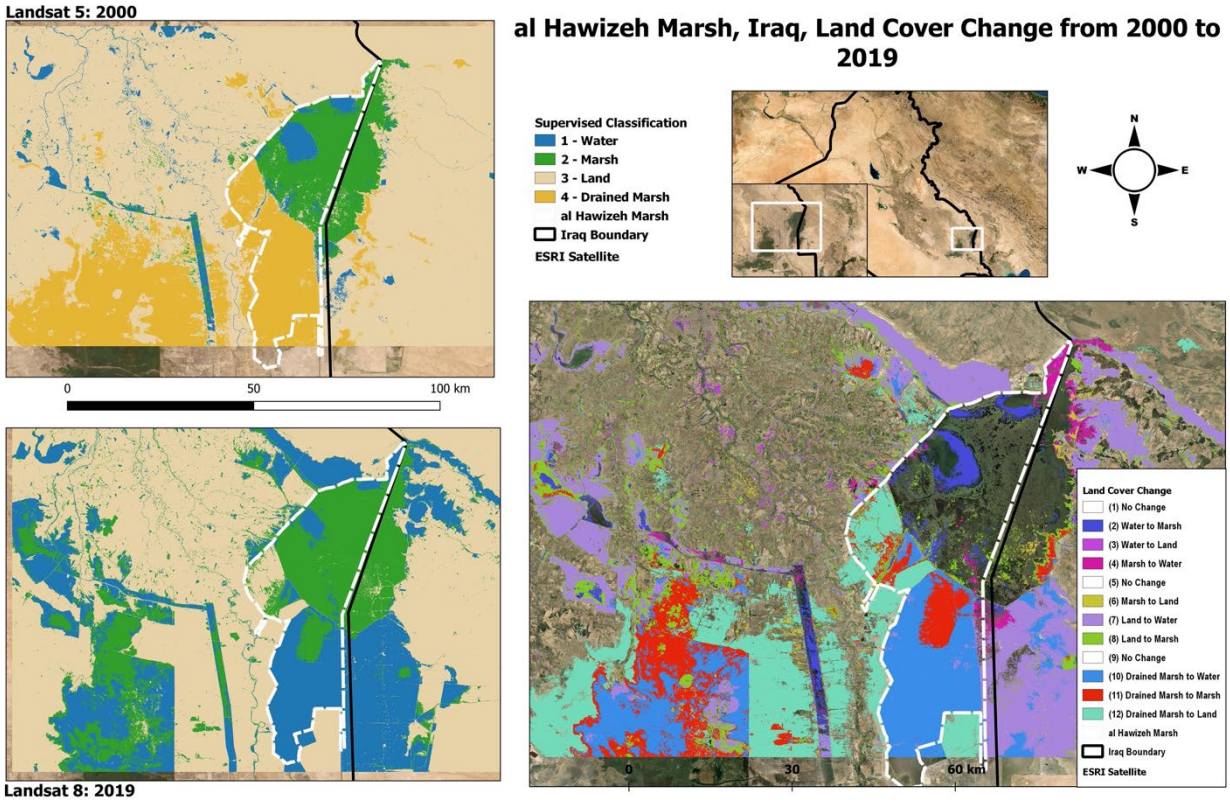

***Figure 2**: Supervised Classification results for Landsat 5 (top) and Landsat 8 (bottom) of the al Hawizeh Marsh. A land change detection analysis was performed to visualize the change and no change within the marsh from 2000 and 2019, as shown in the map on the bottom right.*

NDVI & MNDWI

Results from the NDVI and MNDWI (**Figure 3**) analysis showed a striking difference between 2000 and 2019. Vegetation increased across the study extent from 2000 (top left map) to 2019 (bottom left) map. Furthermore, vegetation health also increased, from 0.075 to 0.243 through 0.863. An increase in vegetation health is most apparent within the marsh's extent and towards the southwestern region (bottom left map). The change in distribution of water from 2000 to 2019 is dramatic with an increase in extent and amount by 2019 (bottom right map).

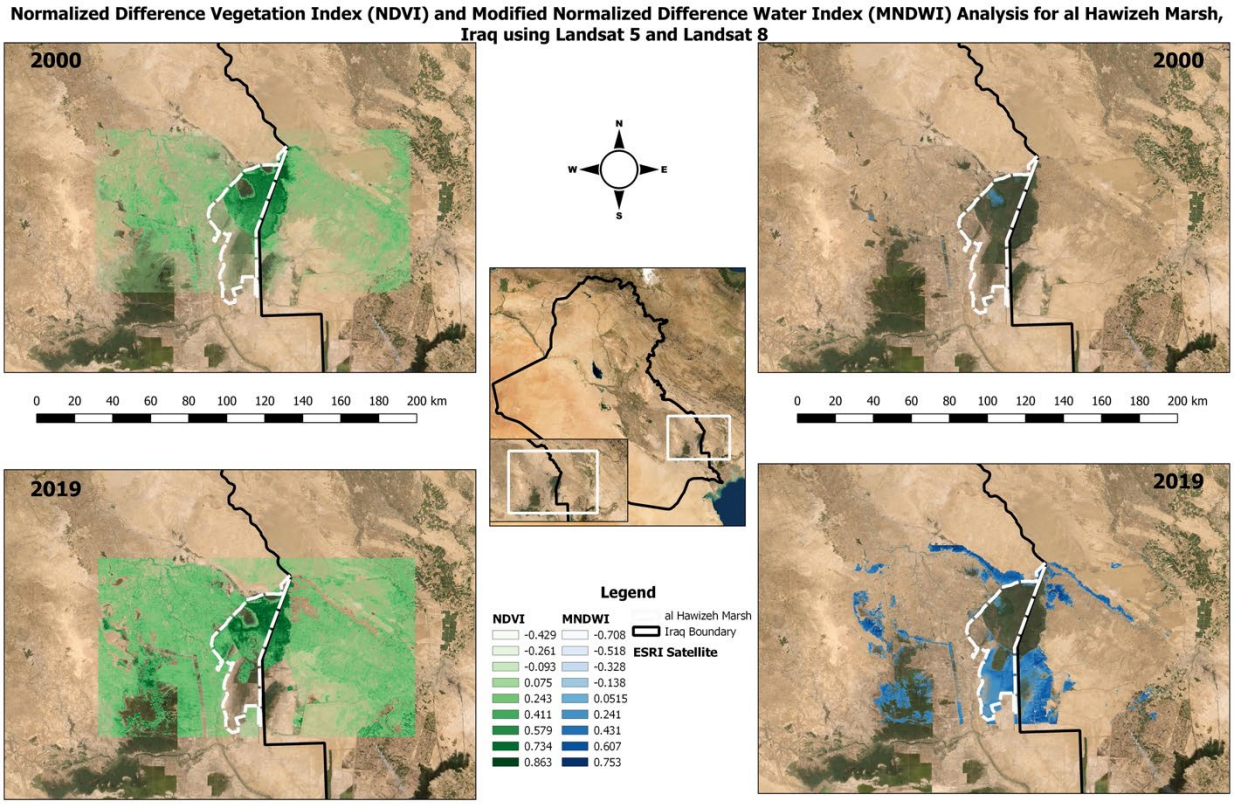

***Figure 3**: NDVI and MNDWI results for Landsat 5 and Landsat 8 spatial images of the al Hawizeh Marsh.*

To further validate this, the Profile Tool (Figures 4 and 5) was employed to assess the dramatic change between the two study years. Landsat 5 is seen in red while Landsat 8 is seen in blue. The few high peaks in Figure 4's Landsat 5 correspond with the vegetation health that is the remnant of the wetland of 2000. In comparison, Landsat 8 shows an overall increase in vegetation health including the first peak corresponding to the newly created wetland in the southwest and its expansion around the al Hawizeh Marsh. The peak drops in NDVI in the center of the profile are a result of decreased vegetation associated with an increase in water in this area. This corresponding trend can be seen in the MNDWI profile in **Figure 5**. In here, the highest peak in Landsat 5 corresponded with the remaining standing water of the marsh of 2000 to the southwest. On the other hand, the highest peaks of Landsat 8 correspond with marsh water gains within the newly expanded extent. These profiles can be found in **Appendix D,** labeled **Figures 15A** and **15B** (NDVI) and **16A** and **16B** (MNDWI).

Figure 4: Landsat 5 (red) and Landsat 8 (blue) NDVI Profile Tool results.

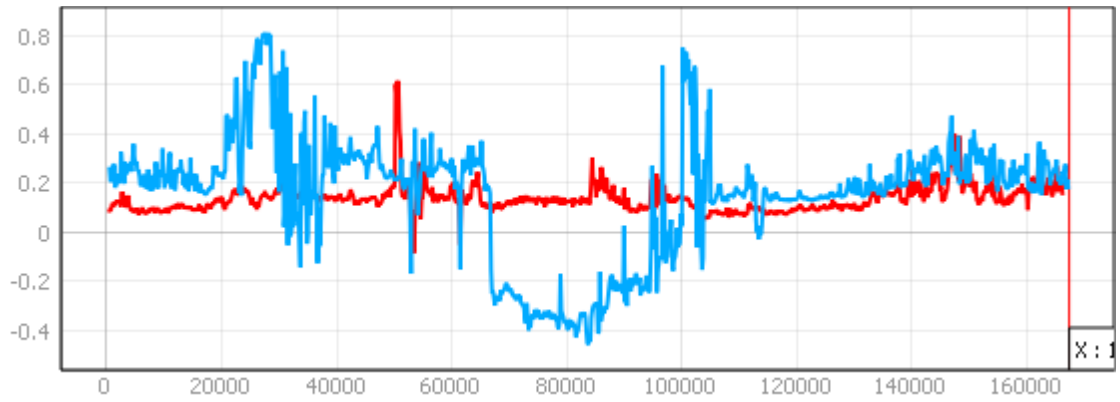

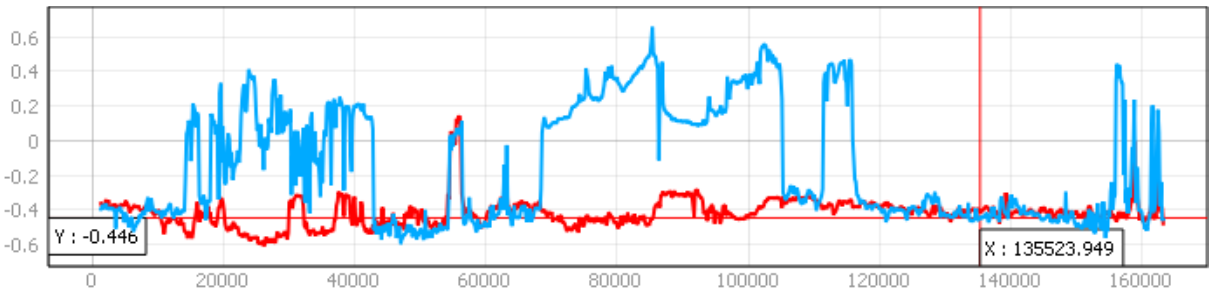

Figure 5: Landsat 5 (red) and Landsat 8 (blue) MNDWI Profile Tool results.

SI & SMMI

Soil salinity and soil moisture show overall increases throughout the study area (**Figure 6**). Soil salinity across the study area increased from 0.148 to 0.655 from 2000 and in 2019 (top and bottom left maps). Within the marsh's extent, soil salinity decreased from 0.221 to 0.0037 as shown in **Figures 3** and **5**. Soil moisture content across the study area depicts an overall increase from 2000 and in 2019. From the 2000 image (top right map), the southern portion of the marsh is shown to have soil moisture content of 0.375 to 0.469, as shown in the bottom right map.

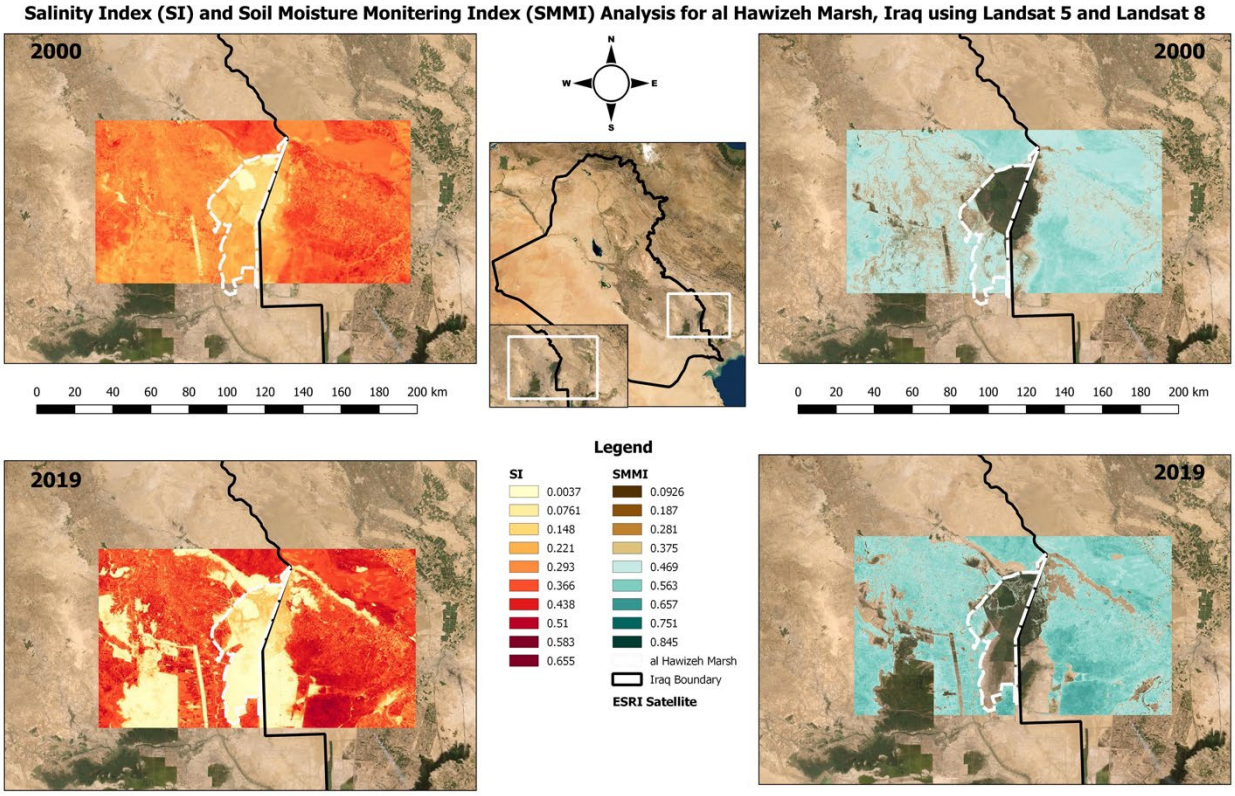

***Figure 6**: SI and SMMI results for Landsat 5 and Landsat 8 spatial images of the al Hawizeh Marsh.*

From the Profile Tool in **Figure 7**, the most notable drop in Landsat 5 corresponds with standing water (i.e., no soil exposed) and vegetation within the canal to the southwest of the study area. The remainder of the study extent, including the southern region of the marsh, however, corresponds with exposed bare soil due to the land and drained marsh classes. In comparison, there are more peaks and drops in the Landsat 8 profile. The peak drops in the Landsat 8 SMMI represent the increase of water and vegetation due to the newly created wetland in the southwest and the extent growth of the al Hawizeh Marsh. The highest peaks, moving from the southwest to the southeast, are associated with exposed bare soil (i.e., land class). This trend is a near replica in the SI profile for Landsat 5 and Landsat 8, as shown in **Figure 8**. The most noticeable drop is situated near the value of 60K on the x-axis and is associated with a decrease in salinity; this corresponds with the standing water found within the canal. High peaks, within Landsat 5, moving from southwest towards the southeast correspond with the presence of high salinity within the study area's land and drained marsh classes. On the other hand, the peak drops in the Landsat 8 profile correspond with the presence of water and vegetation and point towards low salinity concentrations. High peaks, just as with the Landsat 5, possess high salinity and found across the land class across the study area. These profiles can be found in **Appendix D,** labeled **Figures 17A** and **17B** (SMMI), and **18A** and **18B** (SI).

***Figure 7**: Landsat 5 (red) and Landsat 8 (blue) SI Profile Tool results.*

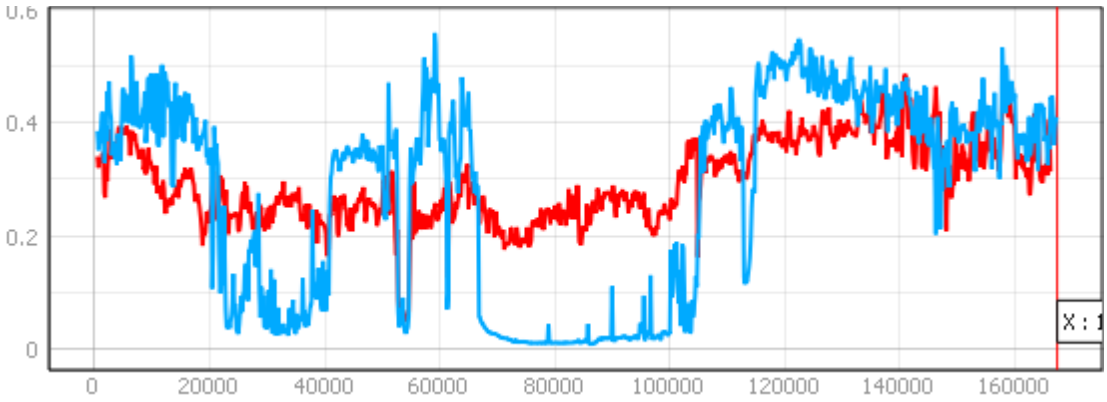

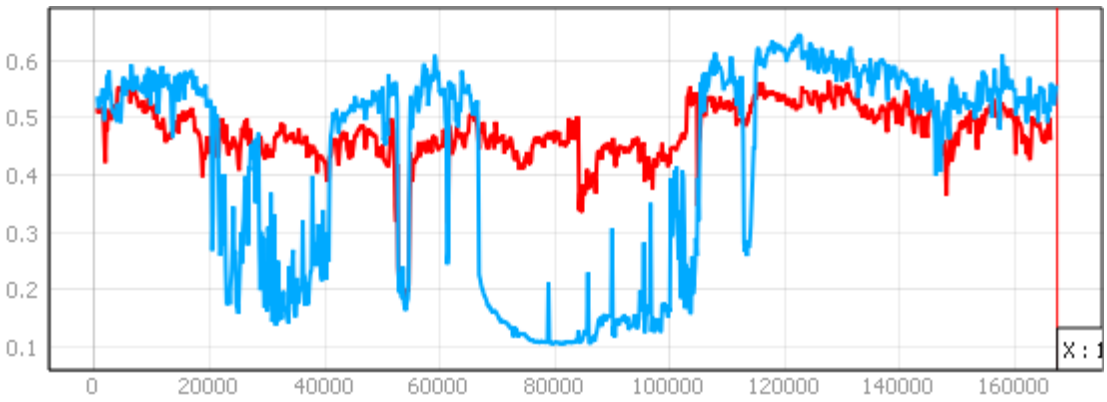

***Figure 8**: Landsat 5 (red) and Landsat 8 (blue) SMMI Profile Tool results.*

LST

Overall, land surface temperatures of this study area showed an increasingly warming trend in 2000 and in 2019. Areas in which the marsh was degraded showed high surface temperatures ranging between 44.5°C to 52.4°C. In contrast, areas with signs of wetland rehabilitation (i.e., increased presence of water and vegetation) revealed decreases in surface temperatures, with a range of 22.4°C to 29.9°C.

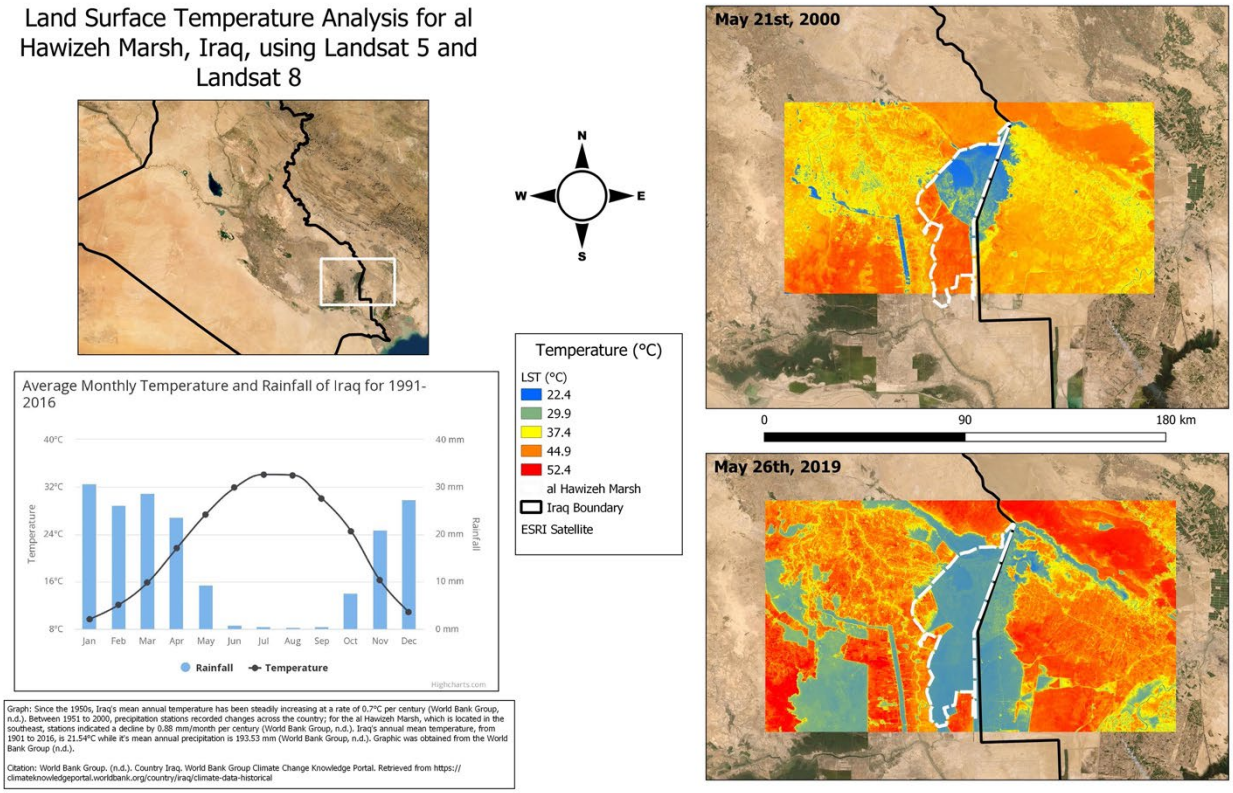

***Figure 9**: LST results for Landsat 5 and Landsat 8 spatial images of the al Hawizeh Marsh.*

The profile of the LST results (**Figure 10**) confirm the variations in temperatures across the study area. The profile of the LST results (**Figure 10**) confirm the variations in temperatures across the study area. In the Landsat 5 (red) and Landsat 8 (blue) profiles, temperature increases are associated with high peaks and low temperatures with low peaks. The first peak drop, which shows moderately low temperatures corresponds with what the supervised classification identified as standing water towards the southwestern corner of the study area. Temperature increases indicate a lack of water and vegetation, corresponding with the drained marsh and land classes. The most apparent peak drop is due to the influence of water within the canal. From the Landsat 8 profile, high peaks correspond with land while low peak drops—most notable from the profile—are associated with the increased water and vegetation within the newly created wetland towards the southwest and the al Hawizeh's marsh extent growth. These profiles can be found in **Appendix D,** labeled **Figures 19A** and **19B**.

Figure 10: Landsat 5 (red) and Landsat 8 (blue) LST Profile Tool results.

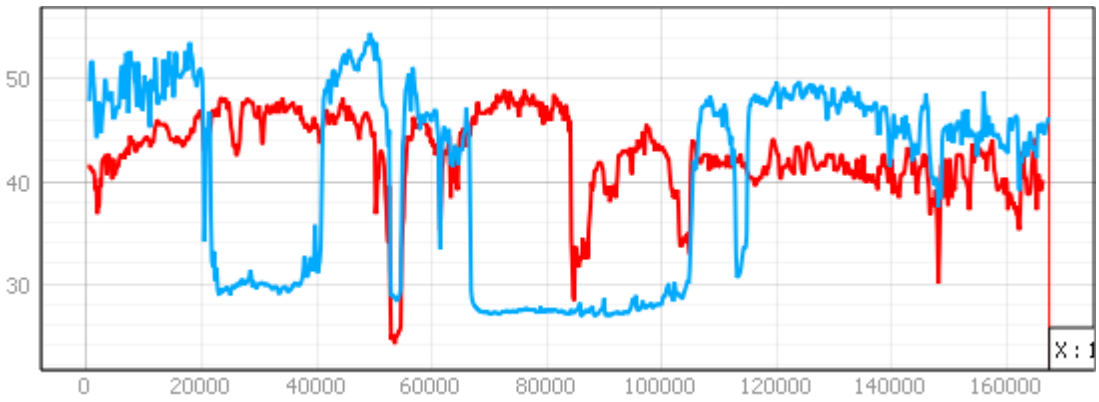

Random Forest Analysis

The random forest model had an out-of-bag (OOB) estimate of error rate of 10.6%. No change was misclassified as Change 15 times with an error rate of 0.057. On the other hand, Change was misclassified as No Change 38 times with an error rate of 0.16. These are shown in **Table 3.**

Table 3: Confusion Matrix for the Random Forest statistical analysis.

Confusion Matrix

	0	**1**	**class.error**
0	248	15	0.05703422
1	38	199	0.16033755

A variable importance plot was produced from the Random Forest model which ranked variables based on importance in model accuracy for the model as well as for determining variable importance for No Change and Change for the al Hawizeh Marsh extent. This is shown in **Figure 11** below.

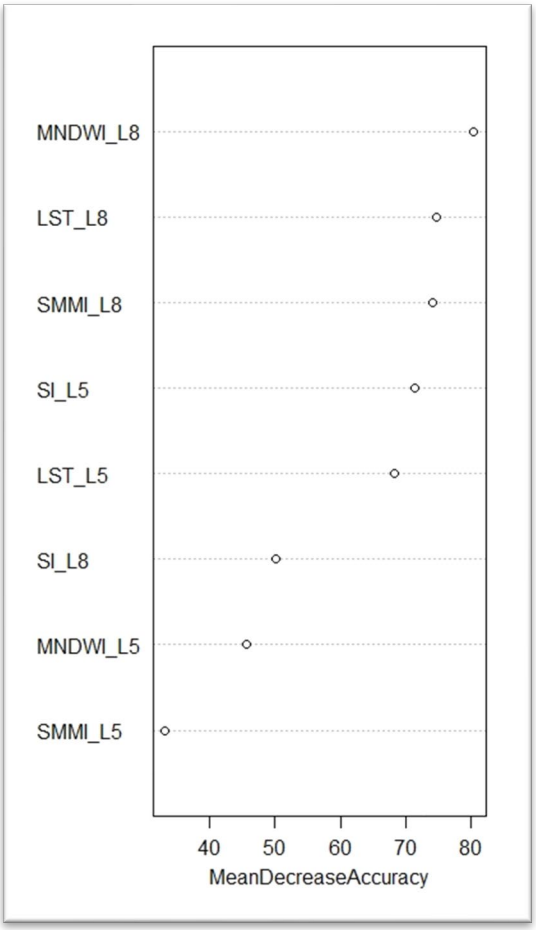

***Figure 11**: Variable Importance results from the al Hawizeh Marsh based on the Random Forest run.*

Important variables plots were generated individually to assess which variables were most important in determining whether an area exhibited change or no change in land cover type between 2000-2019. No Change ranked LST_L8 (71.8%), SMMI_L8 (70.9%) and MNDWI_L8 (70.9%) as the most important variables determining whether no change in land cover occurred between the two time periods.This is seen in **Figure 12**.

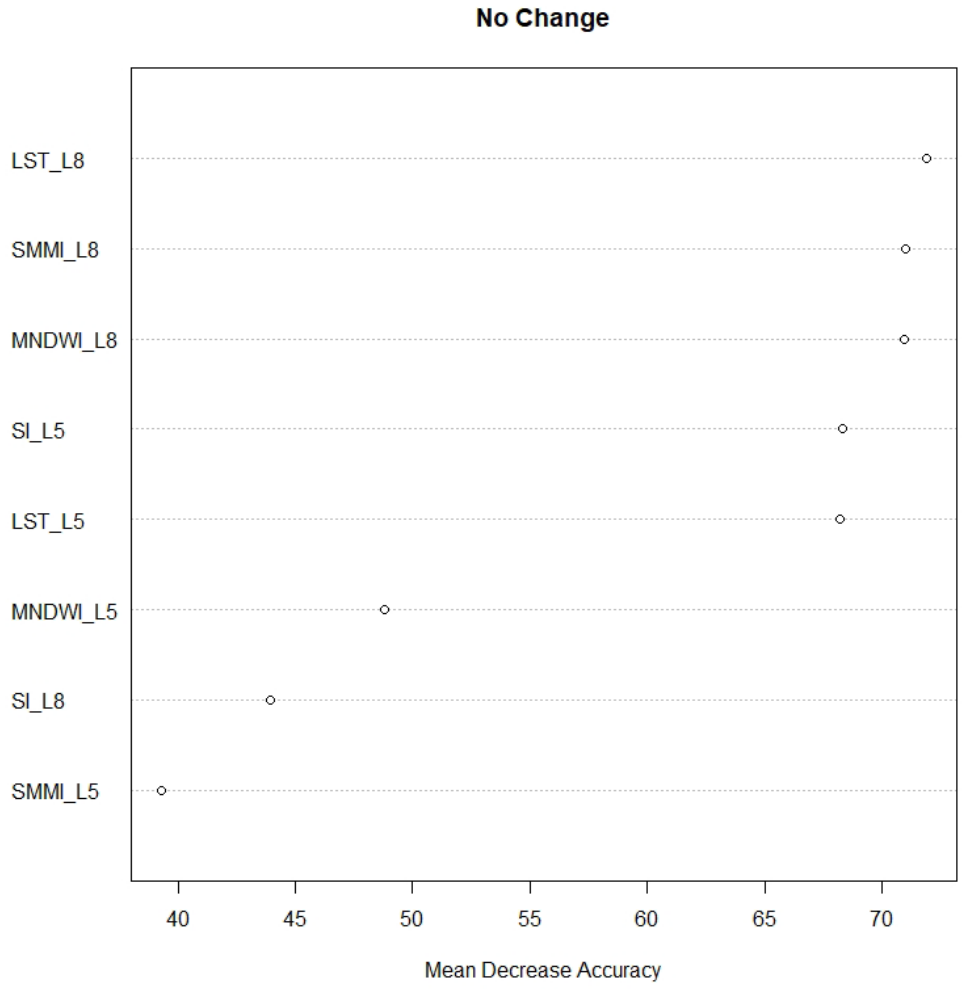

***Figure 12**: Results from the Mean Decrease Accuracy most important variables for No Change within the al Hawizeh Marsh.*

On the other hand, MNDWI_L8 (45.6%), SMMI_L8 (29.0%), and LST_L8 (28.7%) were the most important determinants in change in land cover between the two time periods, as shown in **Figure 13**.

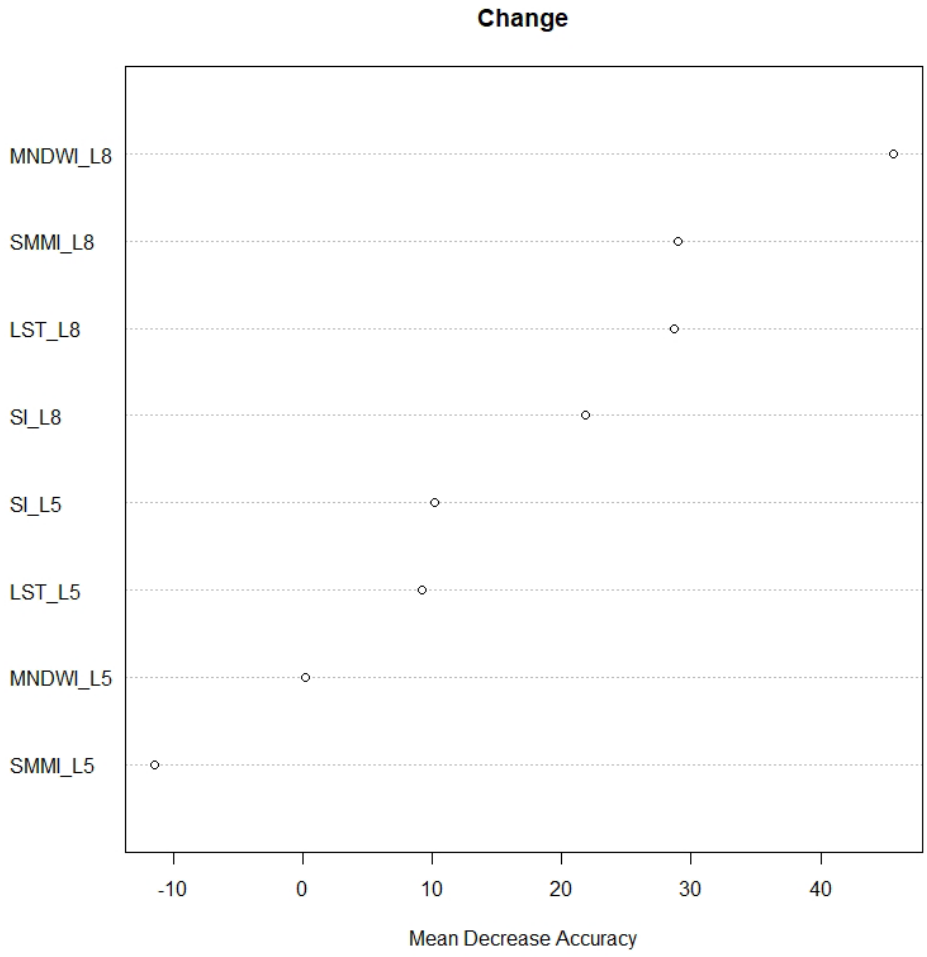

***Figure 13**: Results from the Mean Decrease Accuracy most important variables for Change within the al Hawizeh Marsh.*

In **Figure 14-A**, the water availability of this study area ranged from -0.5 (dry) to 0.5. (wet). Dry areas, with a range of -0.5 to 0, across the study area were indicative of no changes in land cover between 2000 to 2019. Wet areas, with a range of greater than 0, were indicative of land cover changes. In **Figure 14-B**, the soil moisture content of the study area ranged from 0.1 to 0.6. Areas that underwent no land cover change resulted in more drying, with a range of 0.3 to 0.6 from 2000 to 2019. Wetter areas, with a value range of 0.1 to 0.3, were indicative of land cover changes. Finally, in **Figure 14-C**, the land surface temperature of this study area ranged from 25°C to 55°C. In response to no change in land cover between 2000 through 2019, temperatures were warmer, ranging from 40°C to 55°C. On the other hand, change in land cover resulted in temperature decreases, ranging from 25°C to 40°C. The results from all three partial dependence plots are indictive of the conversion of bare ground and the drained wetland areas of the study area into wetland and water land cover types.

A.

No Change

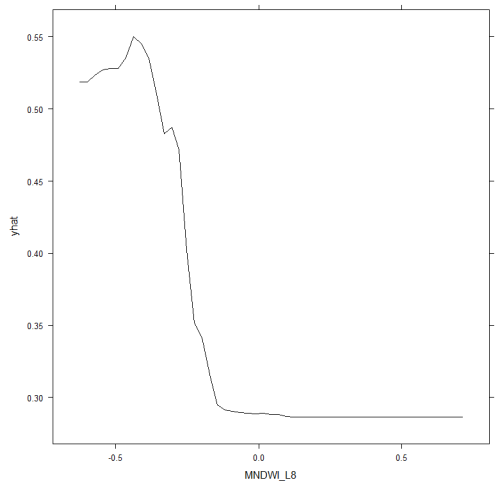

Change

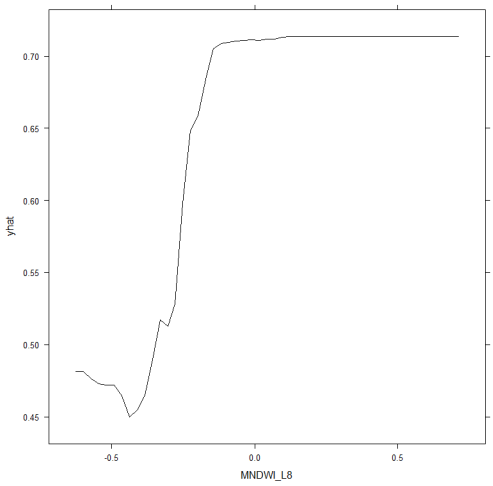

B.

No Change

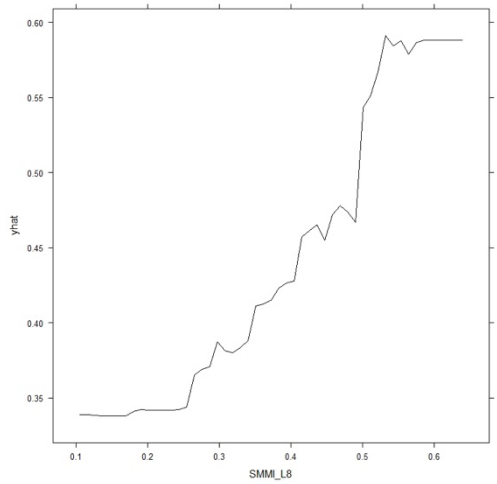

Change

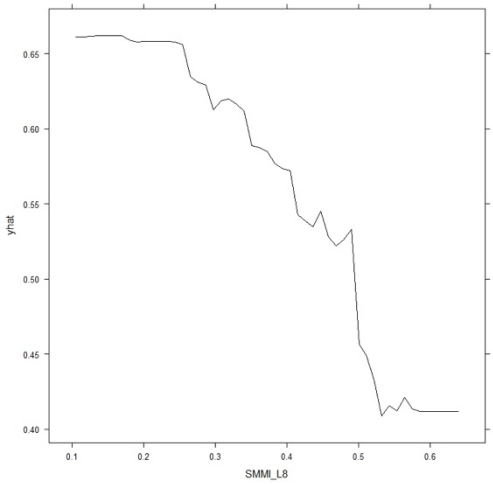

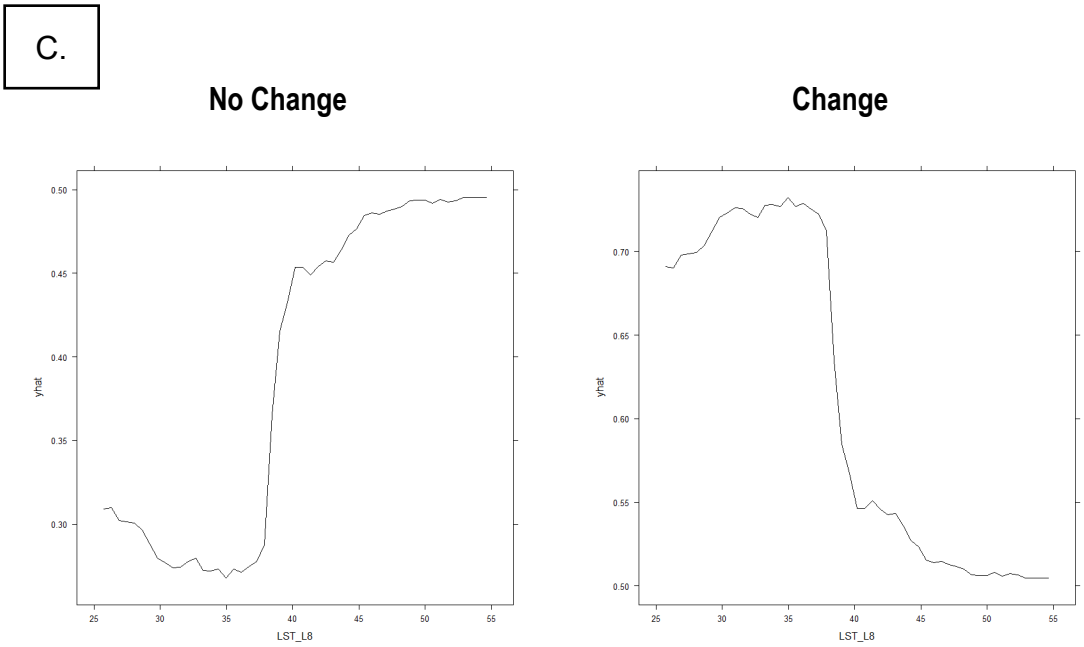

***Figure 14**: Partial Dependence Plots (PDP) for the top 3 most important Change variables, MNDWI_L8 (A), SMMI_L8 (B), and LST_L8 (C).*

Discussion

It was hypothesized that the al Hawizeh Marsh study area will see overall increases in vegetation, water availability, soil moisture content, soil salinity, and land surface temperatures from the study periods of 2000 and 2019. All the results obtained from this project have confirmed this hypothesis. The variable analyses and the random forest model point towards on conclusion. The presence of water, in response to the 2003 reflooding efforts, as given the study area the ability to enter some form of restoration and rehabilitation stage from its intentional degradation and increased wetland extent. Vegetation, soil moisture, soil salinity and surface temperatures were dependent on the existence of water throughout the study area.

The results from the Random Forest validated and emphasized the importance of water availability within the marsh and throughout the study area. The MNDWI (**Figures 3** and **5**) showed increased availability of water and its subsequent changes in land cover types. From 2000 to 2019, bare ground and drained marsh land cover changed into wetland and marsh land cover types. Reflooding efforts led to an associated increase in wetland extent, decrease in salinity, decrease in soil moisture, and decrease in land surface temperatures within these wetland areas. On the other hand, areas where a lack of moisture availability was evident, no change in land cover occurred. The resultant no change in land cover type was indicative of increased soil moisture (i.e., dryness), soil salinity, and land surface temperatures. This was evident in the bare ground and developed land cover types.

The NDVI analysis is similar; it reflects live green vegetation which can be considered an indicator of health, but it does not differentiate between native, non-native, and invasive plant species. Vegetation extent and density increased throughout the study area, in response to the increased presence of water. This was particularly true within the marsh's extent. Per Nature Iraq (2017), a local environmental NGO, *Phragmites australis* is the most abundant of plant species within the marsh. However, they also note that this site is species-rich as defined by the type of habitat: inland standing water-aquatic communities-rooted submerged vegetation, rooted floating vegetation, and free-floating vegetation habitat type; marsh vegetation-halophytic vegetation-reed beds, reed mace beds, and *Schoenoplectus* beds habitat type; and riparian vegetation habitat type, and woodland-shrubs habitat type (Nature Iraq, 2017). This, of course, does not account for an invasive, alien, or non-native species that may have made the marsh their new home during the study periods. To reiterate, while this analysis provided insight on the health of the vegetation, it did indicate the type of marsh vegetation.

The increase in water certainly promoted vegetation growth throughout the study area while there were mixed results for soil salinity, as evident by the SI analysis results shown in **Figures 6** and **7**. Increased soil salinity was attributed to bare ground and developed areas whereas decreases were indicative of the water and marsh areas. An observed salinity hotspot was located near the southwestern corner of the study area. Here, the Euphrates is the main source of water and unlike the Tigris, it is exposed to seawater intrusion from the Persian Gulf (Richardson & Hussain, 2006). As a result of this seawater intrusion, the Euphrates possess a higher salinity concentration. In comparison, the Tigris, and its tributaries, are freshwater (Richardson & Hussain, 2006). Thus, the resultant decrease in soil salinity within the al Hawizeh's marsh extent can be attributed to the re-introduction of freshwater and its ability to dilute salinity concentrations. The decrease in soil salinity within the marsh can be attributed to Tigris as freshwater diluted the salinity concentrations. Maintaining salinity concentrations within an ecosystem is vital to promoting normal biodiversity functions (Cañedo-Argüelles et al., 2018). If the concentration of salinity increases, for example, species richness—fitness and survival—can be adversely affected (Cañedo-Argüelles et al., 2018). A shift in the normal osmotic pressures allows for saline to move down its concentration gradient (move from an area of high concentration to an area of low concentration) and into the cells of plants and wildlife (Cañedo-Argüelles et al., 2018). When this occurs, normal cellular functionality can be reduced or worse, altogether stop (Cañedo-Argüelles et al., 2018).

Soil moisture within the study showed an overall increase in the bare ground and developed areas while showing decreases within the marsh's extent. This result makes sense as exposed bare soil of 2000 was converted into wetland and marsh land cover types in 2019. Soil moisture is dependent on the availability of water (**Figure 13**). This is particularly true for the areas of the marsh, such as the southern extent, that were drained (**Figure 2**). As water and vegetation reclaimed the drained marsh, bare soil moisture decreased; this was shown in the profile of **Figure 8**. However, the rate in which the marsh can retain soil moisture is not uniform as noted by Fitzpatrick (2004) and Richardson and Hussain (2006). When these soils were placed under stress due to forceful burning and draining, sulfuric acid began to form as the soil was directly exposed to oxygen (Fitzpatrick 2004; Richardson & Hussain, 2006). Iraq's famed fertile soils

have become oxidizing hotspots; fostering toxic conditions which the Iraqis unknowingly encouraged their spread once reflooding events took place (Fitzpatrick, 2004; Richardson & Hussain, 2006).

Finally, climate change is responsible for increases in global temperatures and Iraq is no exception. Results from the LST analysis (**Figure 10**) showed an increasing surface temperature across the study. Those areas of increased LST were correlated with bare ground and developed areas. Urban heat islands (UHI) are associated with increasing temperatures. However, surface temperature within the marsh itself has decreased in 2019 compared to its 2000 values. Temperature decreases within the marsh are attributed to the increased water and marsh vegetation which provide a cool and shaded environment.

Conclusion & Future Implications

The results from this project painted a narrative that errs on the side of cautious optimism in response to the 2003 reflooding efforts of Iraq's famed and critically important ecoregion. The obtained results are merely a reflection of spatial analyses with no ground truth to validate the assessed variables. Furthermore, this project focused on only two data points in time, 2000 and 2019. Increasing the timeframe—and accounting for seasonal variations—may reveal different results, one that reflects the country's current environmental conditions.

Thus far, the only published, in-depth ecological assessment was performed from 2003 to 2005 by Richardson and Hussain (2006). As pointed out in the study area section, the al Hawizeh is the only remaining natural wetland of Iraq due to the influence of the Karkhe River (Richardson & Hussain, 2006; AlMaarofi et al., 2014; Ameen et al., 2019). This freshwater source, from Iran, has allowed this site to retain some of its natural biodiversity and water chemistry; however, it should be noted that this protection was only granted to the northern most region of the marsh (AlMaarofi et al., 2014; Ameen et al., 2019). In comparison, its southern reaches, as evident in the spatial analysis results, were drastically transformed due to environmentally destructive ambitions (AlMaarofi et al., 2014; Ameen et al., 2019). An updated ecological assessment must be conducted to improve current knowledge on the health status of this marsh. Of course, ecological assessments must be carried out to the Central and al Hammar Marshes as well; data obtained from the al Hawizeh Marsh can used as the new restoration baseline. As this project only assessed two points in time, additional data can reveal a different story. Results from an updated ecological assessment can improve the conclusions drawn from this spatial analysis.

While the MNDWI assessed wet and dry areas of the study area, it does not provide information on the quality of the water. A study by Hassan et al. (2010), for example, exposed the negative impacts of military operations on a critically important ecosystem. The presence of the military bases and operations resulted in concentrations of cobalt and arsenic at 20,892 µg/g and 3,353 µg/g (Hassan et al., 2010). Additional heavy metals found in this wetland's southern extent include lead, copper, cadmium, and chromium (Hassan et al., 2010). Hassan et al. (2010), note that reflooding efforts have contaminated the al Hawizeh Marsh due to the increase of water and sediments which embedded these heavy metals. This also does not consider the impending and on-going consequences from oil development in the al Hawizeh's

southern reaches, both from Iraq and Iran (Nature Iraq, 2017). The Hawizeh's water quality is also affected from upstream sewage and from increased urban and commercial development (Nature Iraq, 2017). Thus, it is imperative that water assessments must be conducted for the Tigris and Euphrates, and their tributaries, to evaluate the water quality and its impacts on vegetation health and wildlife. If this task is not properly carried out, then it can lead to the degradation of the wetland.

While these bearable temperatures within this ecosystem may be a source of positive news, global climate models (GCMs) project Iraq's mean annual temperature to increase by 2°C by 2050 (World Bank Groups, n.d.[2]). Likewise, Iraq's mean annual rainfall is projected to decrease by 9% by 2050, especially in the months of December, January, and February (World Bank Group, n.d.[2]; Ministry of Foreign Affairs, 2018). While these results only show the surface temperatures for the two study dates, they seem to follow the overall predicted increasing trend for the study area. Decreased precipitation can impact the water volume of the rivers, resulting in a reduced water flow into the wetlands, only for water losses to increase due to evapotranspiration because of increased surface temperatures. In a country that is facing growing water insecurities, its semi-arid climate makes it susceptible to increased occurrences and frequencies of droughts and in turn, accelerates the desertification process (Mahmood Agha & Sarlak, 2016; Ministry of Foreign Affairs, 2018). In a recent example, Iraq encountered a devastating drought, from 2007 to 2009, which halted all restoration efforts into the marshes to preserve the dangerously low volumes of water within the Tigris and Euphrates (Yao, 2013).

Predictions for the future of this study area hinges on the availability of water across the country. Water was, unsurprisingly, the most crucial factor for this project. If there is no water, vegetation decreases while soil salinity, soil moisture content, and land surface temperatures will increase. Climate change is exacerbating the desertification process in this semi-arid region resulting in prolonged droughts. These, as noted earlier, hinder, and counteract any positive restoration efforts. Conservation issues of this region stem from the 90 km embankment Iran constructed on the Iraq/Iran border (Nature Iraq, 2017). This embankment has bisected the al Hawizeh Marsh in half, impacting the biodiversity and water flow of the Karkhe River that knows no boundaries (Nature Iraq, 2017). Iran also pumped water with high salinity concentrations directly into the al Hawizeh Marsh in 2010 and 2011 (Nature Iraq, 2017). On the Iraqi side, the government has oil development plans for the northern and southern regions of the marsh (Nature Iraq, 2017). Additional conservation threats result from the growing urban, rural, and commercial development and expansion near the marsh (Nature Iraq, 2017). This has promoted unsustainable fishing, bird hunting, and increased pollution (e.g., sewage) from upstream sources (Nature Iraq, 2017).

The al Hawizeh Marsh has and will continue to undergo environmental changes exacerbated by anthropogenic consequences. Protection, offered by Ramsar and UNESCO World Heritage Sites, is not enough to ensure the survival of this critically important ecoregion. Nature Iraq (2017) notes that while these is a management plan, it has yet to be implemented. Iraq needs to improve its international treaty efforts with Turkey, Syria, and Iran to guarantee their water security. Furthermore, Iraq must actually begin implementing conservation assessments and

monitoring efforts in the marshes. Environmental policies and laws must be enforced—with outlined penalties—within the country and those of its neighbors, as it safeguards the future of the wetland and all biodiversity it encompasses.

It’s rather simple: if there is no water, there is no marsh.

Acknowledgements

I would like to give a heartful thank you to my mentor and the most amazing professor, Dr. Rachel Isaacs, who provided me with unwavering guidance, patience, and emotional support to ensure the successful completion of this project. My gratitude for you, Dr. Rachel, knows no bounds. I would also like to thank Dr. Dan Zachary for giving me the opportunity to explore this project and for his assistance throughout the project. I am also deeply grateful for his patience with me as I worked on this capstone. Finally, I would like to give a personal thank to my cat, Leonidas, who was the ultimate lap warmer and source of unwavering (at least, it seemed so) emotional support when QGIS decided it didn't want to work.

References

Abdul-Kareem A.K., Al-Timim A., and Al-Jumaily K. (2013). Estimated the Seasonal Change of Temperature in Iraq Using GIS Techniques. *Iraqi Journal of Science* 54(4): pp. 975-982. Retrieved from https://pdfs.semanticscholar.org/ 7101/6a3b1dfdfed6b572f601a5d5d83b0b72f32d.pdf

Aqrawi A.A.M., Jassim S. Z. and Buday T. (2006). Chapter 15: Quaternary Deposits in *Geology of Iraq*. Brno: Dolin, Prague, and Meravian Museum. [PDF].

Albarakat R., and Lakshmi V. (2019). Monitoring Dust Storms in Iraq Using Satellite Data. *Sensors (Basel, Switzerland)* **19**(17): 3687. Retrieved from https://doi.org/10.3390/s19173687

AlMaarofi S.S., Douabul A.A.Z., Warner B.G., and Taylor W.D., (2014). Phosphorus and nitrogen budgets of the Al-Hawizeh marshland after re-flooding. Hydrobiologia 721: pp. 155-164. Retrieved from DOI 10.1007/s10750-013-1657-8

Al Ameri I.D.S., Briant R.M., and Engels S. (2019). Drought severity and increased dust storm frequency in the Middle East: a case study from the Tigris-Euphrates alluvial plain, central Iraq. *Weather* **74**: pp. 416-426. Retrieved from https://doi.org/10.1002/wea.3445

Al-Ansari N.A. (2013). Management of Water Resources in Iraq: Perspectives and Prognoses. *Engineering* 5: pp. 667-684. Retrieved from http://www.scirp.org/pdf/ ENG_2013080616381893.pdf

Al-Ansari N. And Knutsson S. (2011). Possibilities of Restoring the Iraqi Marshlands Known as the Garden of Eden. *Water and Climate Change in the MENA-Region Adaptation, Mitigation, and Best Practices International Conference*. Berlin, Germany. Retrieved from https://www.diva-portal.org/smash/get/diva2:1013359/ FULLTEXT01.pdf

Al-Muqdadi S.W.H. (2019). Developing Strategy for Water Conflict Management and Transformation at Euphrates-Tigris Basin. *Water* **11**(10): 2037. Retrieved from https://doi.org/10.3390/w11102037

Al-Thahaibawi B.M.H., Younis K.H., and Al-Mayaly, I.K.A. (2019). Fish Assemblage Structure in Al-Huwaizah marsh southern of Iraq after inscribed on the World Heritage List. *Iraqi Journal of Science* **60**(7): pp. 1430–1441. Retrieved from doi:10.24996/ijs.2019.60.7.3.

Al-Zaidy K.J.L., Parisi G., Abed S.A., Salim M.A. (2019). Classification of The Key Functional Diversity of the Marshes of Southern Iraq Marshes. *Journal of Physics: Conference Series* **1294**(072021). Retrieved from DOI:10.1088/1742-6596/1294/7/072021

Al-Azzawi S.N. (2016). The deterioration of environmental and life quality parameters in Iraq since the 2003 American occupation of Iraq. *International Journal of Contemporary Iraqi Studies* **10**(1+2): 53-72. Retrieved from DOI: 10.1386/ ijcis.10.1-2.53_1

Ameen F., AlMaarofi S., Talib A., Almansob A., and Al-Homaidan A.A. (2019). Phytoplankton diversity recovers slowly and Cyanobacteria abundance remains high after the reflooding of drained marshes. *Hydrobiologia* **843**: pp. 79-92. Retrieved from https://doi.org/10.1007/s10750-019-04039-6

Aoki C., Al-Lami A., and Kugaprasatham S. (2011). Lessons learned from environmental management of the Iraqi marshlands in the post-conflict period. *Water International* 36(2): pp. 197-206. DOI: 10.1080/02508060.2011.561770

CFR. (2019). The Iraq War. *Council on Foreign Relations*. Retrieved from https:// www.cfr.org/timeline/iraq-war

Dohrmann M. and Hatem R. (2014). The Impact of Hydro-Politics on the Relations of Turkey, Iraq, and Syria. *Middle East Journal* **68**(4): 567-583. Retrieved from: https:// www.jstor.org/stable/43698183

Duys R. (2013). Climate Change, Energy & Natural Resource Management. *United Nations Development Program*. Retrieved from https://www.iq.undp.org/content/ iraq/en/home/library/environment_energy/publication_1.html

Ellis S. (2019). Why Iraq's great rivers are drying. *Vox*. Retrieved from https://]www.vox.com/videos/2019/7/3/20681084/iraq-water-rivers-crisis-drought-isis-war

Elhag M. (2016). Evaluation of Different Soil Salinity Mapping Using Remote Sensing Techniques in Arid Ecosystems, Saudi Arabia. *Journal of Sensors,* article ID 7596175. Retrieved from https://doi.org/10.1155/2016/7596175

FAO. (2016). Euphrates *Tigris. Food and Agricultural Organization of the United Nations AQUASTAT*. Retrieved from http://www.fao.org/nr/water/aquastat/ countries_regions/profile_segments/euphrates.tigris-WR_eng.stm

Fitzpatrick R.W. (2004). Changes in soil and water characteristics of some natural, drained and re-flooded soils in the Mesopotamian marshlands: Implications for land management planning. *CSIRO Land and Water: Client Report*. Retrieved from http://www.clw.csiro.au/publications/consultancy/2004/Mesopotamian- marshlands-soil.pdf

Garstecki T., and Amr Z. (2011). Biodiversity and Ecosystem Management in the Iraqi Marshlands — Screening Study on Potential World Heritage Nomination. Amman, Jordan: IUCN. Retrieved from https://www.iucn.org/content/biodiversity- and-ecosystem-management-iraqi-marshlands-screening-study-potential-world- heritage-nomination

GIS & RS Solution. (2020[1]). Calculating Land Surface Temperature (LST) of Landsat 7 and Landsat 5 | ArcGIS Tutorial. *YouTube*. Retrieved from

https://www.youtube.com/watch?v=4tG7mr2_mdc&t=314s&ab_channel=GIS%26RSSolution

GIS & RS Solution. (2020[2]). Estimating Land Surface Temperature Landsat 8 | ArcGIS Tutorial | 2020. *YouTube.* Retrieved from https://www.youtube.com/watch?v=5AaF0-yakb8

Hameed M., Ahmadalipour A., and Moradkhani H. (2018). Apprehensive Drought Characteristics over Iraq: Results of a Multidecadal Spatiotemporal Assessment. *Geosciences* **8**(2)**:** 58. Retrieved from https://doi.org/10.3390/geosciences8020058

Hamdan M.A., Asada T., Hassan F.M., Warner B.G., Douabul A., Al-Hilli M.R.A. and Alwan A.A. (2010). Vegetation Response to Re-flooding in the Mesopotamian Wetlands, Southern Iraq. *Wetlands* **30**: pp. 177-188. https://doi.org/10.1007/ s13157-010-0035-9
Harris L. and Taylor A.H. (2015). Topography, Fuels, and Fire Exclusion Drive Fire Severity of the Rim Fire in an Old-Growth Mixed-Conifer Forest, Yosemite National Park, USA. Ecosystems 18: pp. 1192-1208. Retrieved from DOI: 10.1007/s10021-015-9890-9

Hasab H.A., Jawad H.A., Dibs H., Ussain H.M. and Al-Ansari N. (2020). Evaluation of Water Quality Parameters in marshes Zone Southern of Iraq Based on Remote Sensing and GIS Techniques. *Water, Air, & Soil Pollution* **231**(183). Retrieved from https://doi.org/10.1007/s11270-020-04531-z

Hassan F.M., Al-Haidarey M.J.S., Al-Kubaisey A.R.A., and Douabul A.A.Z. (2010). The Geoaccumulation Index of Some Heavy Metals in Al-Hawizeh Marsh. *Iraq. E-journal of Chemistry* **7**(S1): pp. S157-S162. Retrieved from https://doi.org/ 10.1155/2010/839178

Herbert E.R., Boon P., Burgin A.J., Neubauer S.C., Franklin R.B., Ardón M., Hopfensperger K.N., Lamers L.P.M., and Gell P. (2015). A global perspective on wetland salinization: ecological consequences of a growing threat to freshwater wetlands. *Ecosphere* **6**(10): pp. 1-43. Retrieved from https://doi.org/10.1890/ES14-00534.1

Hussain N.A., Ahmed S.M., and Lazem L.F. (2013). Occurrence and Abundance of Fish Larvae in the restored Mesopotamian Marshlands, Southern Iraq. Journal of King Abdulaziz University: *Marine Sciences* **24**(2): pp. 15–27. Retrieved from DOI: 10.4197/Mar. 24-2.2

Lv J., Jiang W., Wang W., Wu Z., Liu Y., Wang X., and Li Z. (2019). Wetland Loss Identification and Evolution Based on Landscape and Remote Sensing Indices in Xiong'an New Area. *Remote Sensing* **11**(23): 2842. Retrieved from https://www.mdpi.com/2072-4292/11/23/2834

Masboob H. (2019). Visualizing the Changes of a Vanishing Mesopotamia: The Al- Hawizeh Marsh, Iraq. *AS.420.703 Open Source GIScience for Environmental Research, JHU Course*. Summer 2019. Unpublished documentation.

Masboob H. (2020). A Mesopotamian Story: Impacts of the Reflooding Efforts on the Iraqi

Marshland's Biodiversity. *AS.420.611 Ecology, JHU Course.* Fall 2020. Unpublished documentation.

Mastrocola P. (2017[1)]. Physical Settings of Marshlands. *Fanack Water*. Retrieved from https://water.fanack.com/specials/iraqi-marshes/physical-setting/

Mastrocola P. (2017[2]). The Marshes in the 20th Century. *Fanack Water*. Retrieved from https://water.fanack.com/specials/iraqi-marshes/marshes-20th-century/

Mastrocola P. (2017[3]). The Marshes in the 21st Century. *Fanack Water*. Retrieved from https://water.fanack.com/specials/iraqi-marshes/the-marshes-21th-century/

Martinez-Taboada F. and Redondo J.I. (2020). The SIESTA (SEAVVA Integrated evaluation sedation tool for anesthesia) project: Initial development of a multifactorial sedation assessment tool for dogs. *PLoS ONE* **15**(4): e0230779. Retrieved from https://doi.org/ 10.1371/journal.pone.0230799

Ministry of Foreign Affairs. (2018). Climate Change Profile Iraq. *Ministry of Foreign Affairs of the Netherlands*. Retrieved from https://reliefweb.int/report/iraq/climate- change-profile-iraq

Mohamed A.R.M., Al-Saboonchi A.A., and Raadi F.K. (2017). Ecological assessment of East Hammar marsh, Iraq using a number of ecological guides. *Journal of King Abdulaziz University: Marine Sciences* **26**(2): pp. 11-22. Retrieved from DOI :10.4197/ Mar.26-2.2

Nature Iraq. 2017. Key Biodiversity Areas of Iraq. Sulaimaniuah Iraq: Tablet House Publishing.

Ramsar. (2015). The "Garden of Eden" in Iraq now internationally protected as Wetlands of International Importance. *Ramsar Convention on Wetlands of International Importance.* Retrieved from https://www.ramsar.org/news/the-garden-of-eden-in-iraq-now-internationally-protected-as-wetlands-of-international

Randell J.R. (2003). Iraq: History. *Scholastic — Teacher's Activity Guide.* Retrieved from http://teacher.scholastic.com/scholasticnews/indepth/iraq/iraq_history.htm

Richardson C.J. (2018) Mesopotamian Marshes of Iraq. In: Finlayson C., Milton G., Prentice R., Davidson N. (eds) The Wetland Book. Springer, Dordrecht. Retrieved from https://doi.org/10.1007/978-94-007-4001-3_70

Richardson C.J. and Hussain N.A. (2006). Restoring the Garden of Eden: An Ecological Assessment of the Marshes of Iraq. *BioScience* **56**(6): pp. 477–489, Retrieved from https://doi.org/10.1641/0006-3568(2006)56[477:RTGOEA]2.0.CO;2

RSIS. (2012[1]). Information Sheet on Ramsar Wetlands. *Ramsar Information Sheet.* Retrieved from https://rsis.ramsar.org/RISapp/files/RISrep/IQ1718RIS.pdf?language=en
RSIS. (2012[2]). Hawizeh Marsh. *Ramsar Sites Information Service*. Retrieved from https://rsis.ramsar.org/ris/1718?language=en

Rubec C. and Young L. (2014). Report on a Ramsar Team Visit to the Hawizeh Marsh Ramsar Site, Iraq. *Ramsar.* Retrieved from https://www.ramsar.org/sites/default/files/documents/library/report_of_ramsar_team_iraq_140815.pdf

Salman S.D., Mohammed F.A., Abdul-Husein M.G., Huda K.A., Anfas N.A., Douabul B.G., and Asada T. (2014). Seasonal changes in zooplankton communities in the re- flooded Mesopotamian wetlands, Iraq. J*ournal of Freshwater Ecology* **29**(3): pp. 397-412. Retrieved from https://doi.org/10.1080/02705060.2014.907547

SER. (n.d.). Iraq: Reviving Eden — The Iraqi Marshlands. *Society for Ecological Restoration*. Retrieved from https://www.ser-rrc.org/project/iraq-reviving-eden-the- iraqi-marshlands/

Singer F.D. (2016). Chapter 11, Section 11.4: How can human-mediated changes to habitat cause species to become endangered, or go extinct? In *Ecology in Action.* Cambridge: Cambridge University Press. [Kindle Edition].

UNEP-WCMC and IUCN (2021), Protected Planet: The World Database on Protected Areas (WDPA) and World Database on Other Effective Area-based Conservation Measures (WD-OECM) [Online], February 2021, Cambridge, UK: UNEP-WCMC and IUCN. Retrieved from www.protectedplanet.net.

UNESCO. (2016). The Marshlands of Iraq Inscribed on UNESCO's World Heritage List. *United Nations Educational, Scientific and Cultural Organization.* Retrieved from http://www.unesco.org/new/en/member-states/single-view/news/the_marshlands_of_iraq_inscribed_on_unescos_world_heritag/

UNESCO. (n.d.). The Ahwar of Southern Iraq: Refuge of Biodiversity and the Relict Landscape of the Mesopotamian Cities. *World Heritage Convention United Nations Educational, Scientific and Cultural Organization.* Retrieved from https://whc.unesco.org/en/list/1481/

UNEP, WMO, UNCCD. (2016). Global Assessment of Sand and Dust Storms. United Nations Environment Programme, Nairobi. Retrieved from https://uneplive.unep.org/redesign/media/docs/assessments/global_assessment_of_sand_and_dust_storms.pdf

USGS. (n.d.[1]). Landsat Surface Reflectance-Derived Spectral Indices Landsat Normalized Difference Vegetation Index. *USGS.* Retrieved from https://www.usgs.gov/core-science-

systems/nli/landsat/landsat-normalized-difference-vegetation-index?qt-science_support_page_related_con=0#qt-science_support_page_related_con

USGS. (n.d.[2]). What are the best Landsat spectral bands for use in my research? *USGS.* Retrieved from https://www.usgs.gov/faqs/what-are-best-landsat-spectral-bands-use-my-research?qt-news_science_products=0#qt-news_science_products

U.S. Geological Survey (USGS) Earth Resources Observation and Science (EROS) Center. 04/05/2012. Landsat ETM+ SLC-off - Path: 166 Row: 38 for Scene: LT05_L1TP_166038_20000521_20161215_01_T1. Remote-Sensing Image. NASA EOSDIS Land Processes DAAC, USGS Earth Resources Observation and Science (EROS) Center, Sioux Falls, South Dakota (https://lpdaac.usgs.gov), accessed January 2021, at https://earthexplorer.usgs.gov/

U.S. Geological Survey (USGS) Earth Resources Observation and Science (EROS) Center. 04/05/2012. Landsat ETM+ SLC-off - Path: 166 Row: 38 for Scene: LC08_L1TP_166038_20190526_20190605_01_T1. Remote-Sensing Image. NASA EOSDIS Land Processes DAAC, USGS Earth Resources Observation and Science (EROS) Center, Sioux Falls, South Dakota (https://lpdaac.usgs.gov), accessed January 2021, at https://earthexplorer.usgs.gov/

U.S. Geological Survey (USGS). 2019. SRTM 1-Arc Second Global (Entity ID: SRTM1N31E047V3, published 20140923), accessed January 2021, at https://earthexplorer.usgs.gov/

Talib A.H. (2017). Some limnological features of Al-Hammar Marsh South of Iraq After Restoration. *The Iraqi Journal of Agricultural Sciences* **48**(5): pp. 1356-1363. Retrieved from https://doi.org/10.36103/ijas.v48i5.345

World Bank Group. (n.d.). Country Iraq. *World Bank Group Climate Change Knowledge Portal.* Retrieved from https://climateknowledgeportal.worldbank.org/country/iraq/vulnerability

World Bank Group. (n.d.[2]). Climate Date > Projections. *World Bank Group Climate Change Knowledge Portal.* Retrieved from https://climateknowledgeportal.worldbank.org/country/iraq/climate-data-projections

Xu H. (2006). Modification of normalized difference water index (NDWI) to enhance open water features in remotely sensed imagery. *International Journal of Remote Sensing* **27**(14): pp. 3025-3033. Retrieved from http://www.aari.ru/docs/pub/060804/xuh06.pdf

Yao J. (2013). Iraq's First National Park: A Story of Destruction and Restoration in the Mesopotamian Marshlands. *Circle of Blue.* Retrieved from https://www.circleofblue.org/2013/world/iraqs-first-national-park-a-story-of-destruction-and-restoration-in-the-mesopotamian-marshlands/

Image References

Mastrocola P. (2017[2]). The Marshes in the 20th Century. *Fanack Water*. Retrieved from https://water.fanack.com/specials/iraqi-marshes/marshes-20th-century/

Mastrocola P. (2017[3]). The Marshes in the 21st Century. *Fanack Water*. Retrieved from https://water.fanack.com/specials/iraqi-marshes/the-marshes-21th-century/

Appendix A

Landsat 5

The Landsat 5 land surface temperatures were calculated from the thermal image Band 6 using the following calculations from the GIS & Solutions (20201) tutorial:

1. **Conversion DN to Radiance**
   a. $L_\lambda = \left(\frac{LMAX_\lambda - LMIN_\lambda}{QCALMAX - QCALMIN}\right) \times (QCAL - QCALMIN) + LMIN_\lambda$
      i. L_λ = Spectral radiance
      ii. $QCAL$ = Quantized calibrated pixel value in DN
      iii. $LMAX_\lambda$ = Spectral radiance scaled to QCALMAX in (Watts/m^2 * sr *μm))
      iv. $LMIN_\lambda$ = Spectral radiance scaled to QCALMAX in (Watts/m^2 * sr *μm))
      v. QCALMIN = Minimum quantized calibrated pixel value (corresponding to $LMIN_\lambda$) in DN
      vi. QCALMAX = Minimum quantized calibrated pixel value (corresponding to $LMAX_\lambda$) in DN = 255

2. **Convert Radiance into Brightness Temperature (BT, In Kelvin)**
   a. $T = \frac{K2}{\ln(\frac{K1}{L_\lambda}+1)}$
      i. T = Effective at-satellite temperature in Kelvin
      ii. $K2$ = Calibration constant 2
      iii. $K1$ = Calibration constant 1
      iv. L_λ = Spectral radiance in (Watts/m^2 * sr *μm))

3. **Convert Degree Kelvin into Degree Celsius**
   a. C = K – 273.15

Landsat 8

The Landsat 8 land surface temperatures were calculated from the thermal image Band 10 using the following calculations from the *GIS & Solutions* (2020[2]) tutorial:

1. **Converting Top of Atmospheric (TOA) Radiance**
   a. $L_\lambda = ML \times Q_{cal} + AL - O_i$
      i. L_λ = TOA spectral radiance (Watts / (m^2 * sr * μm))
      ii. $ML =$ Radiance multiplicative Band (no.)
      iii. AL = Radiance Add Band (no.)

iv. Q_{cal} = Quantized and calibrated standard product pixel value (DN) or band 10
v. O_i = correction value for band 10, value is 0.29

2. Conversion to Top of Atmosphere (TOA) Brightness Temperature (BT)

a. $BT = (\frac{K_2}{\ln(\frac{K_1}{L\lambda+1})- 273.15})$
   i. $BT =$ Top of Atmosphere brightness temperature (°C)
   ii. $L\lambda$ = TOA spectral radiance (Watts / (m^2 * sr * μm))
   iii. K_1 = K_1 Constant Band
   iv. K_2 = K_2 Constant Band

3. Calculate Normalized Difference Vegetation Index

a. $\boldsymbol{NDVI} = \frac{Near\ Infrared\ (NIR) - Red\ Band\ (R)}{Near\ Infrared\ (NIR) + Red\ Band\ (R)}$
b. $\boldsymbol{NDVI} = \frac{(\boldsymbol{Band\ 5 - Band\ 4})}{(\boldsymbol{Band\ 5 + Band\ 4})}$

4. Calculate Land Surface Emissivity (LSE)

a. $PV = (\frac{(NDVI - NDVI_{min})}{(NDVI_{max} + NDVI_{\min})})^2$
   i. PV = Proportion of Vegetation
   ii. NDVI = DN values from NDVI image
   iii. $NDVI_{min}$ = Minimum DN values from NDVI image
   iv. $NDVI_{max}$ = Maximum DN values from NDVI image
b. $E = 0.004 \times PV + 0.986$
   i. E = Land Surface Emissivity
   ii. PV = Proportion of Vegetation
   iii. 0.086 corresponds to a correction value of the equation

5. Land Surface Temperature (LST)

a. $LST = \frac{BT}{(1+(\frac{\gamma \times BT}{c_2}) \times \ln(E))}$
   i. BT = Top of Atmosphere brightness temperature (°C)
   ii. λ = Wavelength of emitted radiance (Band 10 is 10.8 & Band 11 is 12.0)
   iii. E = Land Surface Emissivity
   iv. c_2 = 14388 μm K
      1. $c_2 = h \times \frac{c}{s}$
         a. h = Planck's Constant = 6.626×10^{-34} J s
         b. s = Boltzmann Constant = 1.38×10^{-23} JK
         c. c = Velocity of light = 2.998×10^8 m/s

Appendix B

***Table 4**: Landsat 5 supervised land cover changed based on pixel count.*

Value	Pixel count	Area (m^2)	Acres
(1) Water	540443	486398	120191.736309
(2) Marsh	1065946	959351400	237060.893658
(3) land	11802368	10622131200	2624785.7821703
(4) Drained Marsh	2375977	2138379300	528405.032648

***Table 5**: Landsat 8 supervised land cover changed based on pixel count.*

Value	Pixel Count	Area (m^2)	Acres
(1) Water	3248424	2923581600	722432.7465184
(2) Marsh	2420872	2178784800	538389.4491389
(3) Land	11738360	10564524000	2610550.733039

Appendix C

***Image 3**: Land cover change matrix utilizing L5_Super as the reference classification and L8_Super as the new classification to assess changes within the marsh from 2000 to 2019. These were obtained from QGIS.*

CrossClassCode	NewClass	ReferenceClass	PixelSum	Area [metre^2
1	1.0	1.0	270037.0	243033300.0
4	1.0	2.0	111330.0	100197000.0
7	1.0	3.0	1581106.0	1422995400.0
10	1.0	4.0	862881.0	776592900.0
2	2.0	1.0	196373.0	176735700.0
5	2.0	2.0	871907.0	784716300.0
8	2.0	3.0	683036.0	614732400.0
11	2.0	4.0	483735.0	435361500.0
3	3.0	1.0	74033.0	66629700.0
6	3.0	2.0	82709.0	74438100.0
9	3.0	3.0	9538226.0	8584403400.0
12	3.0	4.0	1029361.0	926424900.0

	> LAND COVER CHANGE MATRIX [metre^2] > NewClass			
V_ReferenceClass	1.0	2.0	3.0	Total
1.0	243033300	176735700	66629700	486398700
2.0	100197000	784716300	74438100	959351400
3.0	1422995400	614732400	8584403400	10622131200
4.0	776592900	435361500	926424900	2138379300
Total	2542818600	2011545900	9651896100	14206260600

Appendix D

NDVI Profile

***Figure 15**: NDVI profile showing high (A) and low (B) peaks in vegetation in Landsat 5 (red) and Landsat 8 (blue) emphasizing Landsat 8 results.*

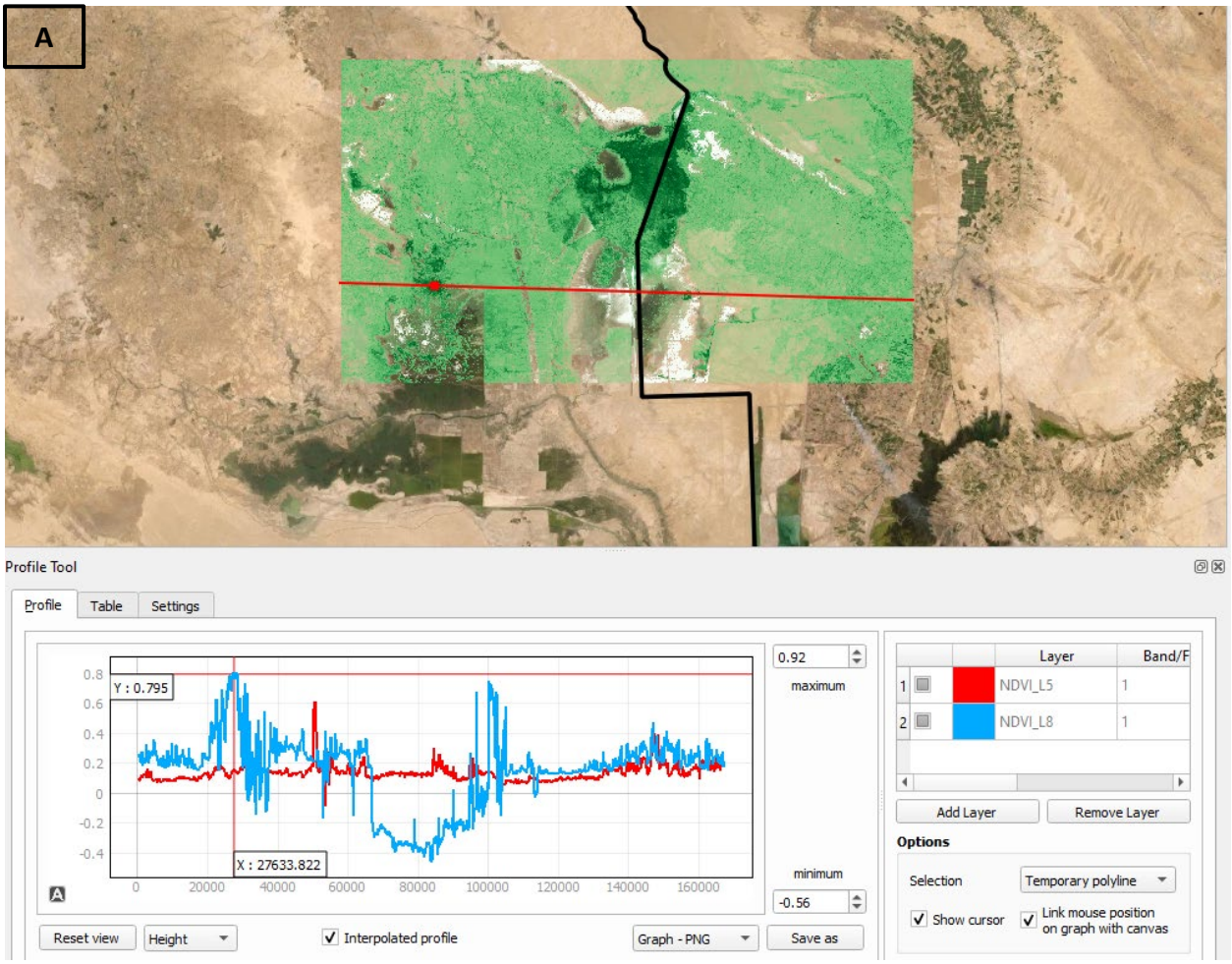

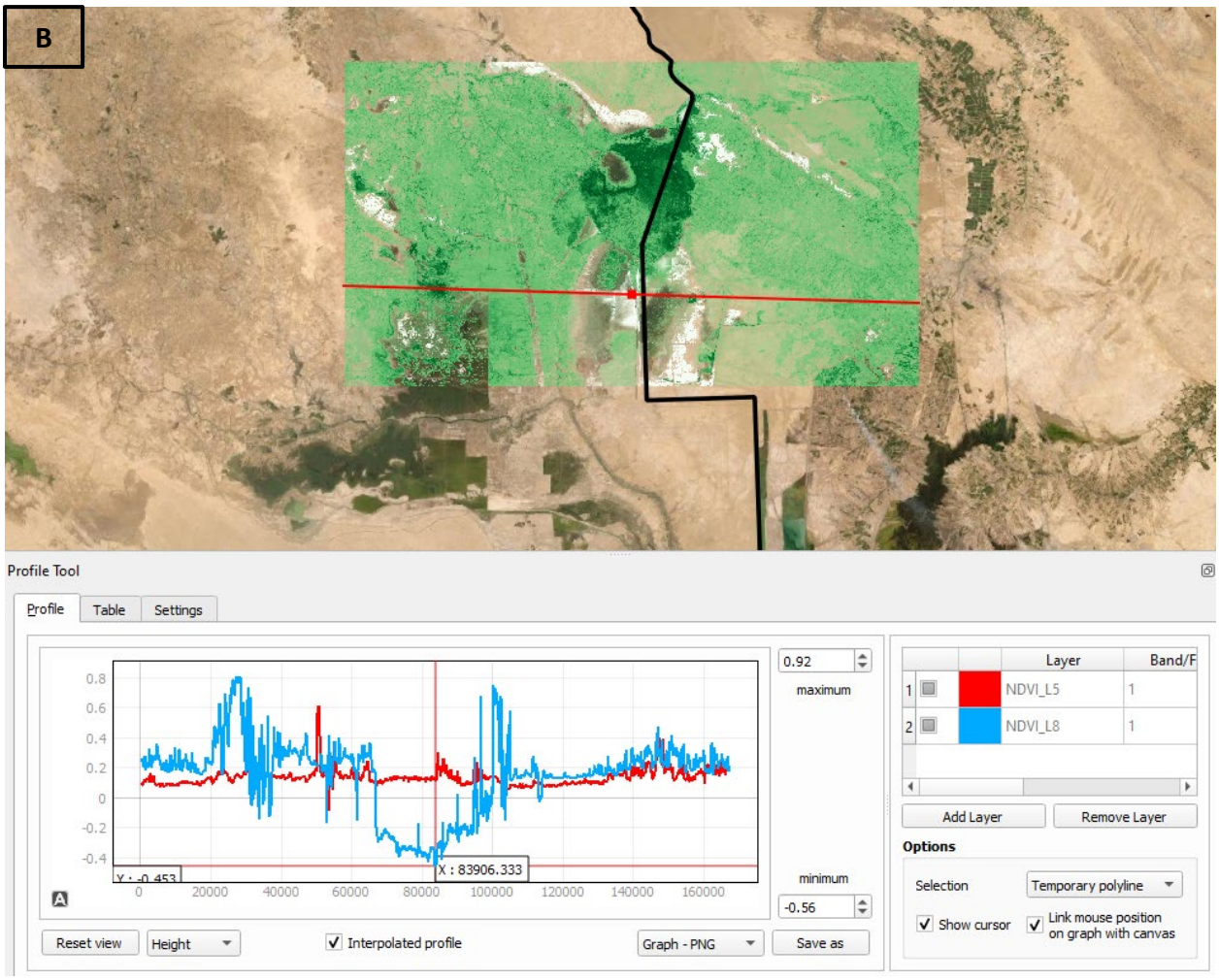
B
Profile Tool
Profile
Table
Settings
0.8
0.6
0.4
0.2
0
-0.2
-0.4
X : -0.453
X : 83906.333
0
20000
40000
60000
80000
100000
120000
140000
160000
0.92
maximum
minimum
-0.56
Reset view
Height
Interpolated profile
Graph - PNG
Save as
Layer
Band/F
1
NDVI_L5
1
2
NDVI_L8
1
Add Layer
Remove Layer
Options
Selection
Temporary polyline
Show cursor
Link mouse position on graph with canvas

MNDWI Profile

***Figure 16**: MNDWI profile showing high (A) and low (B) peaks in water availability in Landsat 5 (red) and Landsat 8 (blue) emphasizing Landsat 8 results.*

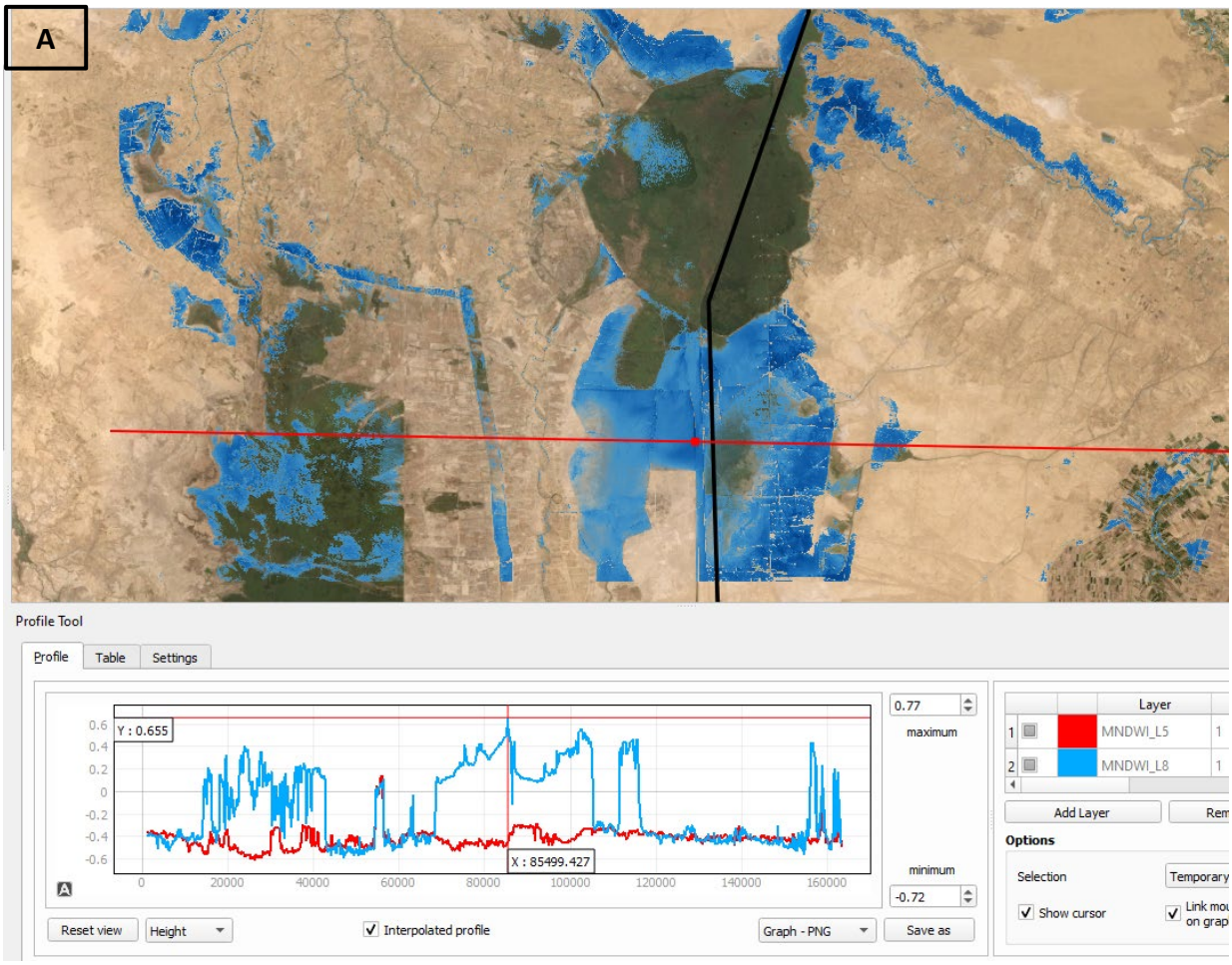

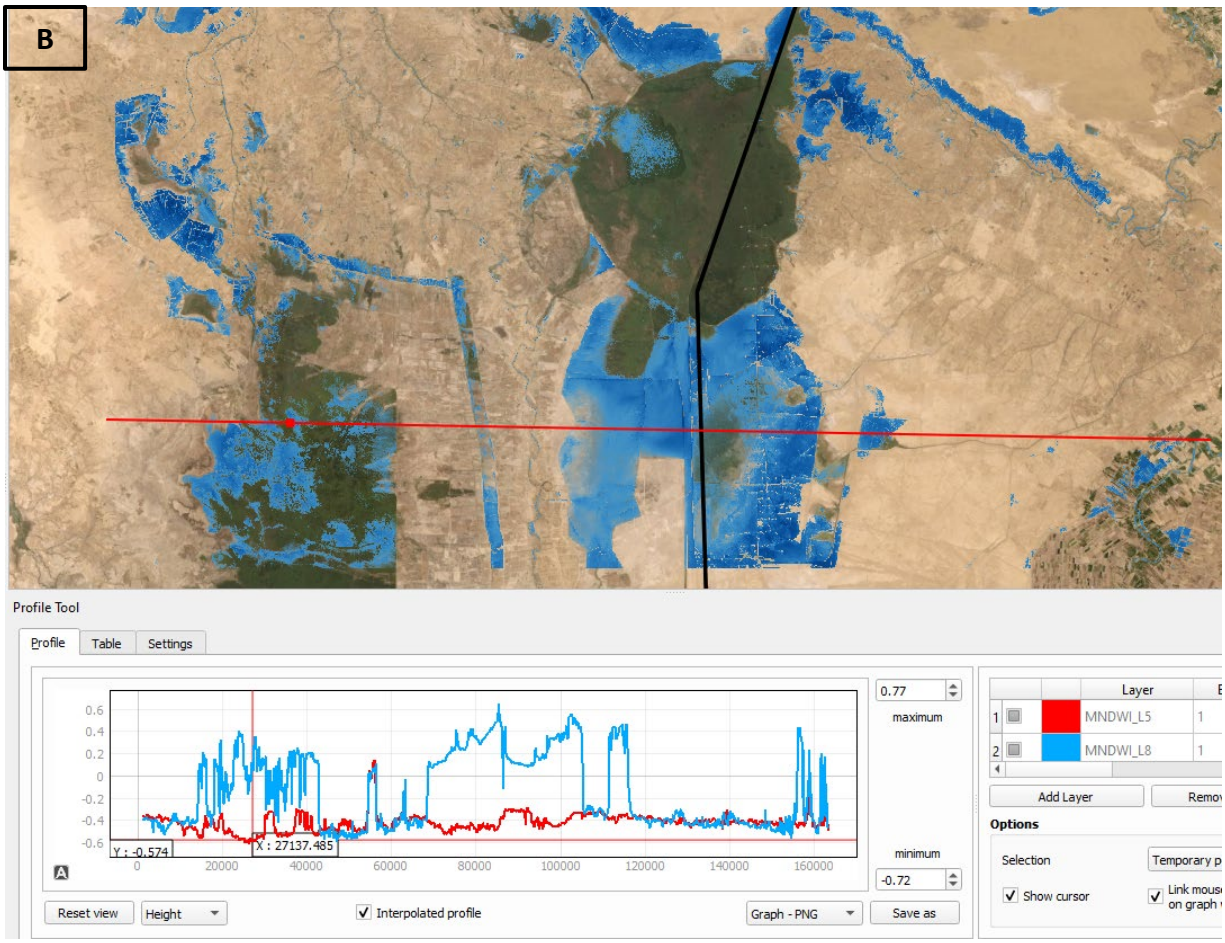
B
Profile Tool
Profile
Table
Settings
0.6
0.4
0.2
0
-0.2
-0.4
-0.6
Y : -0.574
X : 27137.485
0
20000
40000
60000
80000
100000
120000
140000
160000
0.77
maximum
minimum
-0.72
Reset view
Height
Interpolated profile
Graph - PNG
Save as
Layer
1
MNDWI_L5
2
MNDWI_L8
Add Layer
Options
Selection
Show cursor

SMMI Profile

Figure 17: SMMI profile showing high (A) and low (B) peaks in soil moisture content in Landsat 5 (red) and Landsat 8 (blue) emphasizing Landsat 8 results.

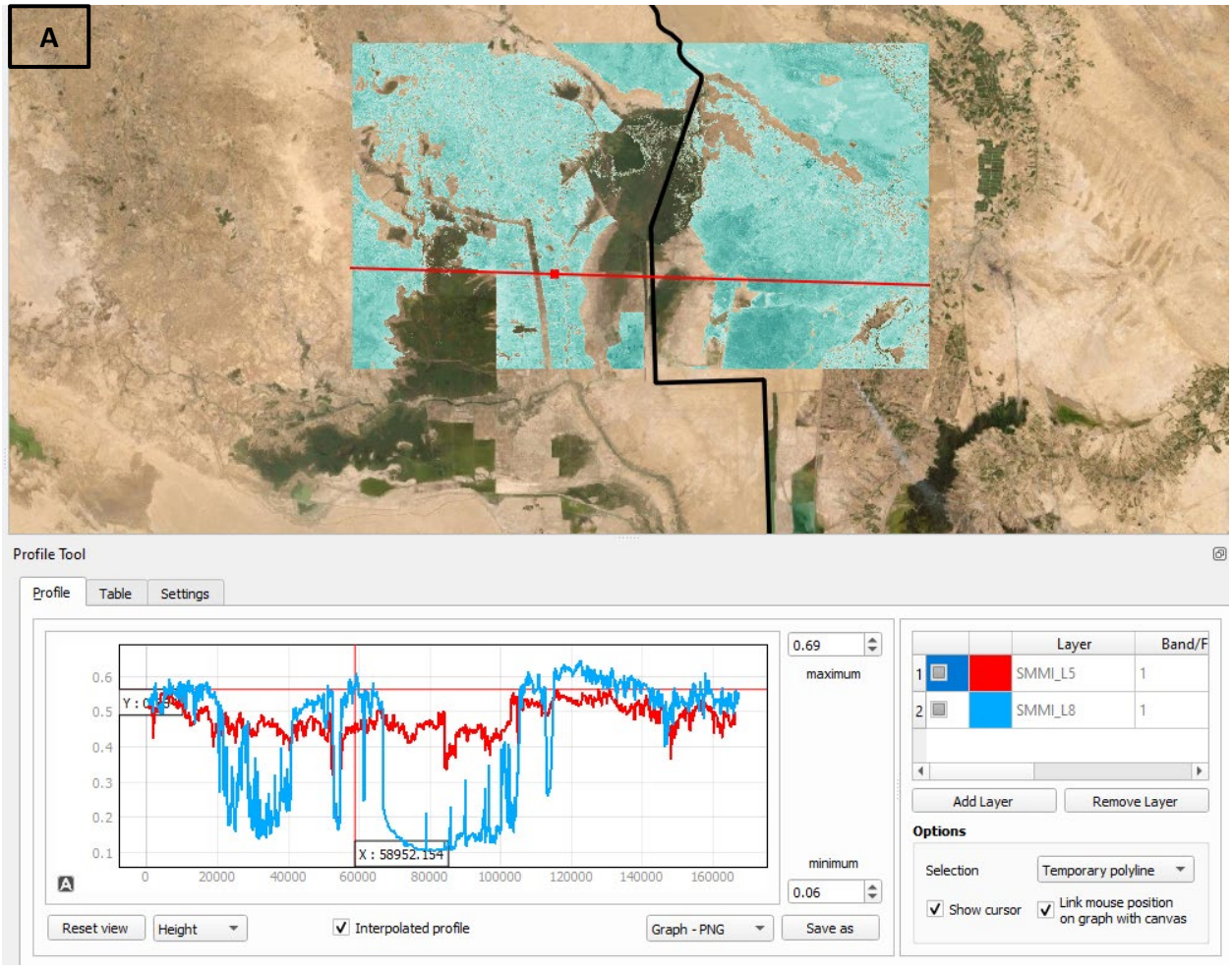

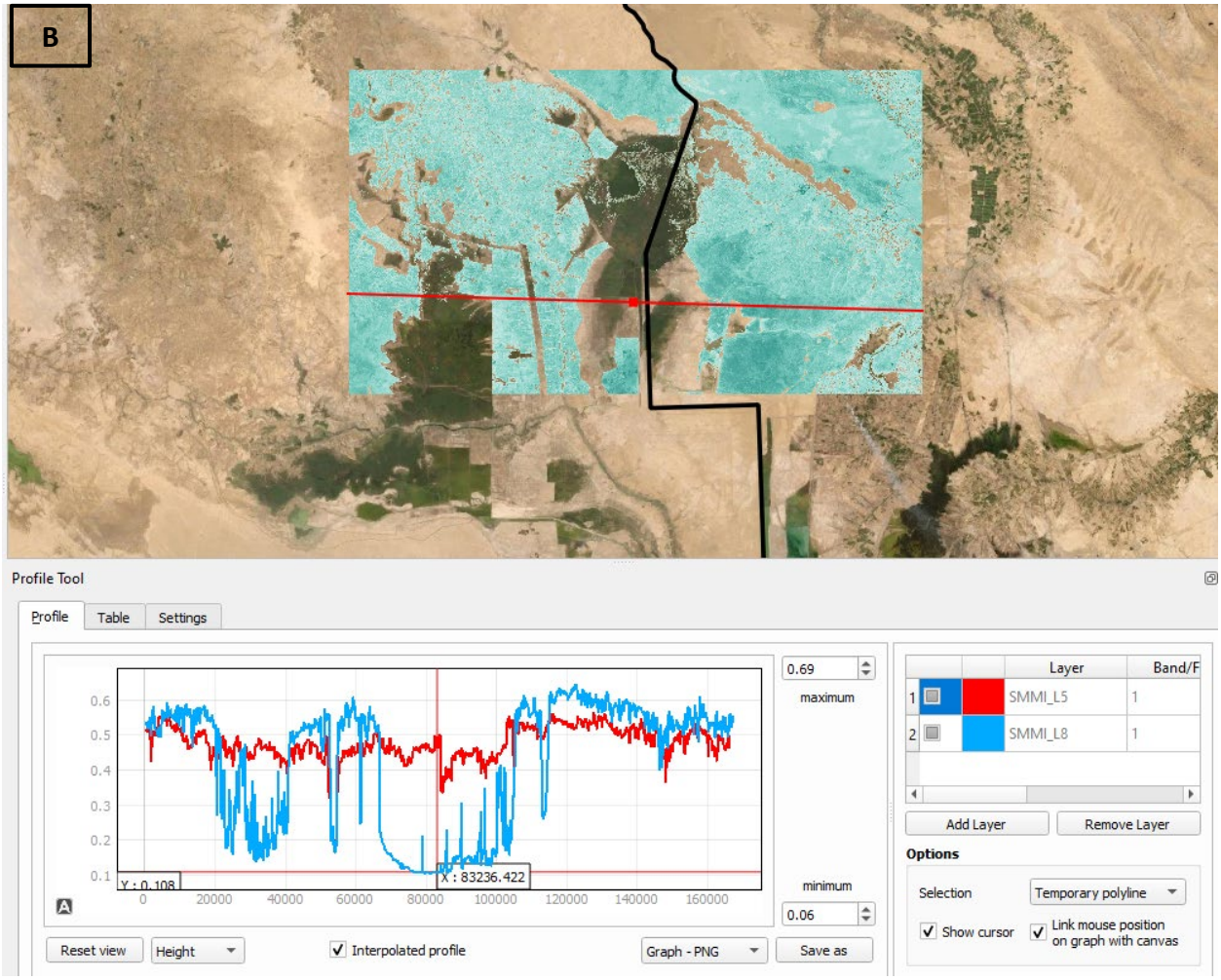
B
Profile Tool
Profile
Table
Settings
0.69
maximum
0.6
0.5
0.4
0.3
0.2
0.1
Y : 0.108
X : 83236.422
0
20000
40000
60000
80000
100000
120000
140000
160000
minimum
0.06
Reset view
Height
Interpolated profile
Graph - PNG
Save as
Layer
Band/F
1
SMMI_L5
1
2
SMMI_L8
1
Add Layer
Remove Layer
Options
Selection
Temporary polyline
Show cursor
Link mouse position on graph with canvas

SI Profile

Figure 18: SI profile showing high (A) and low (B) peaks for soil salinity of Landsat 5 (red) and Landsat 8 (blue) emphasizing Landsat 8 results.

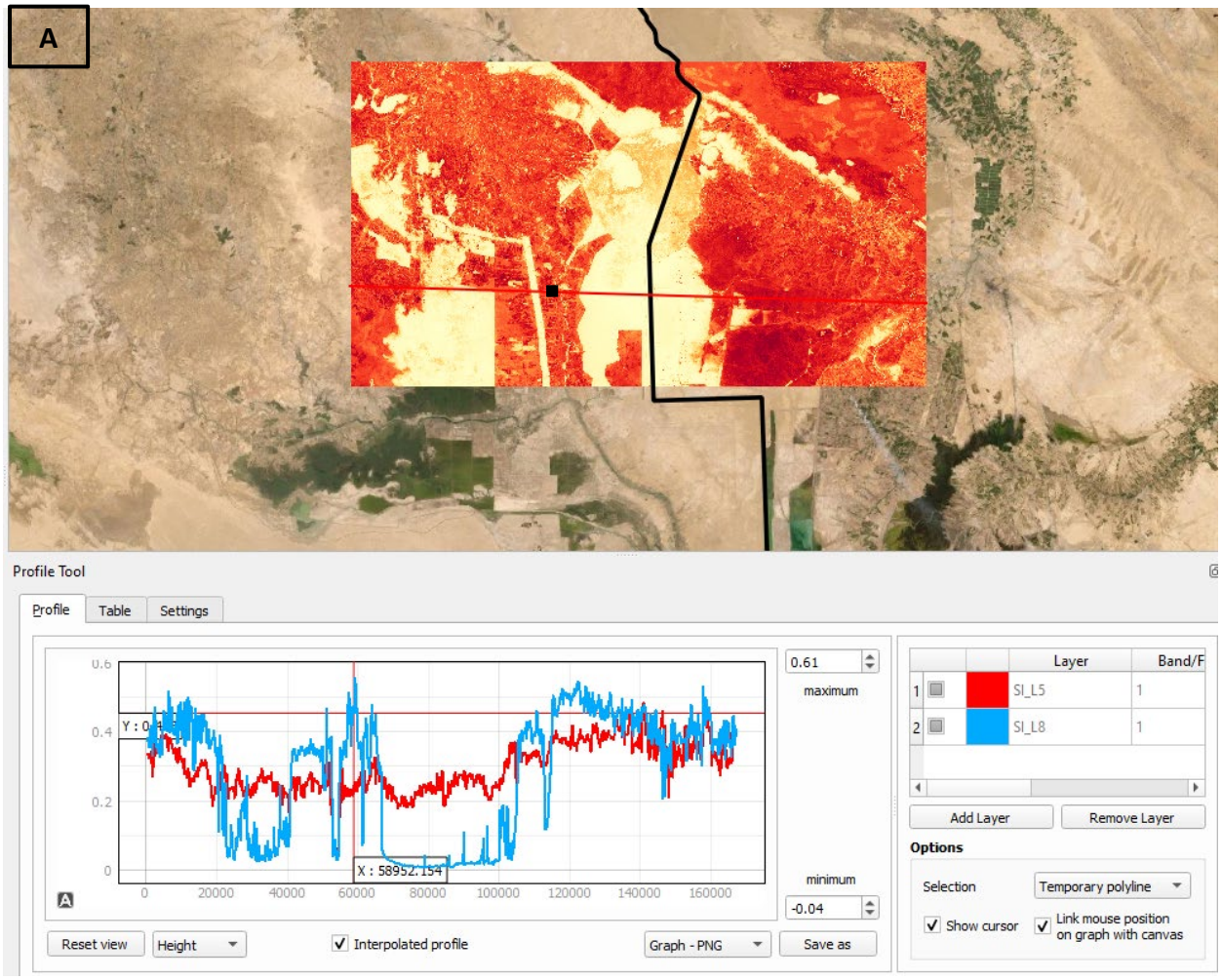

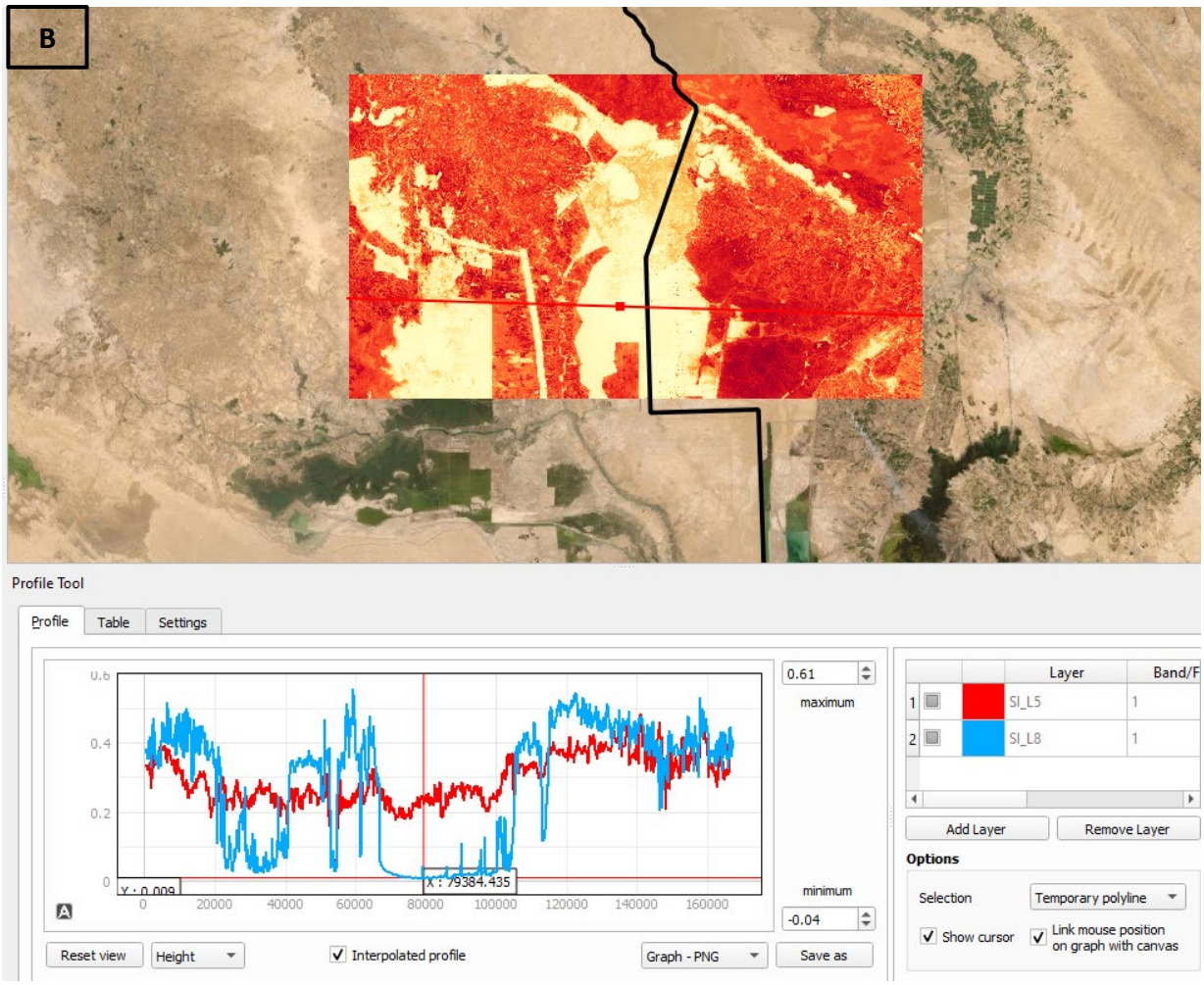
B
Profile Tool
Profile
Table
Settings
0.6
0.4
0.2
0
0
20000
40000
60000
80000
100000
120000
140000
160000
X : 79384.435
0.61
maximum
minimum
-0.04
Layer
Band/F
1
SI_L5
1
2
SI_L8
1
Add Layer
Remove Layer
Options
Selection
Temporary polyline
Show cursor
Link mouse position on graph with canvas
Reset view
Height
Interpolated profile
Graph - PNG
Save as

LST Profile

***Figure 19**: LST profile showing high (A) and low (B) peaks for land surface temperatures of Landsat 5 (red) and Landsat 8 (blue) emphasizing Landsat 8 results.*

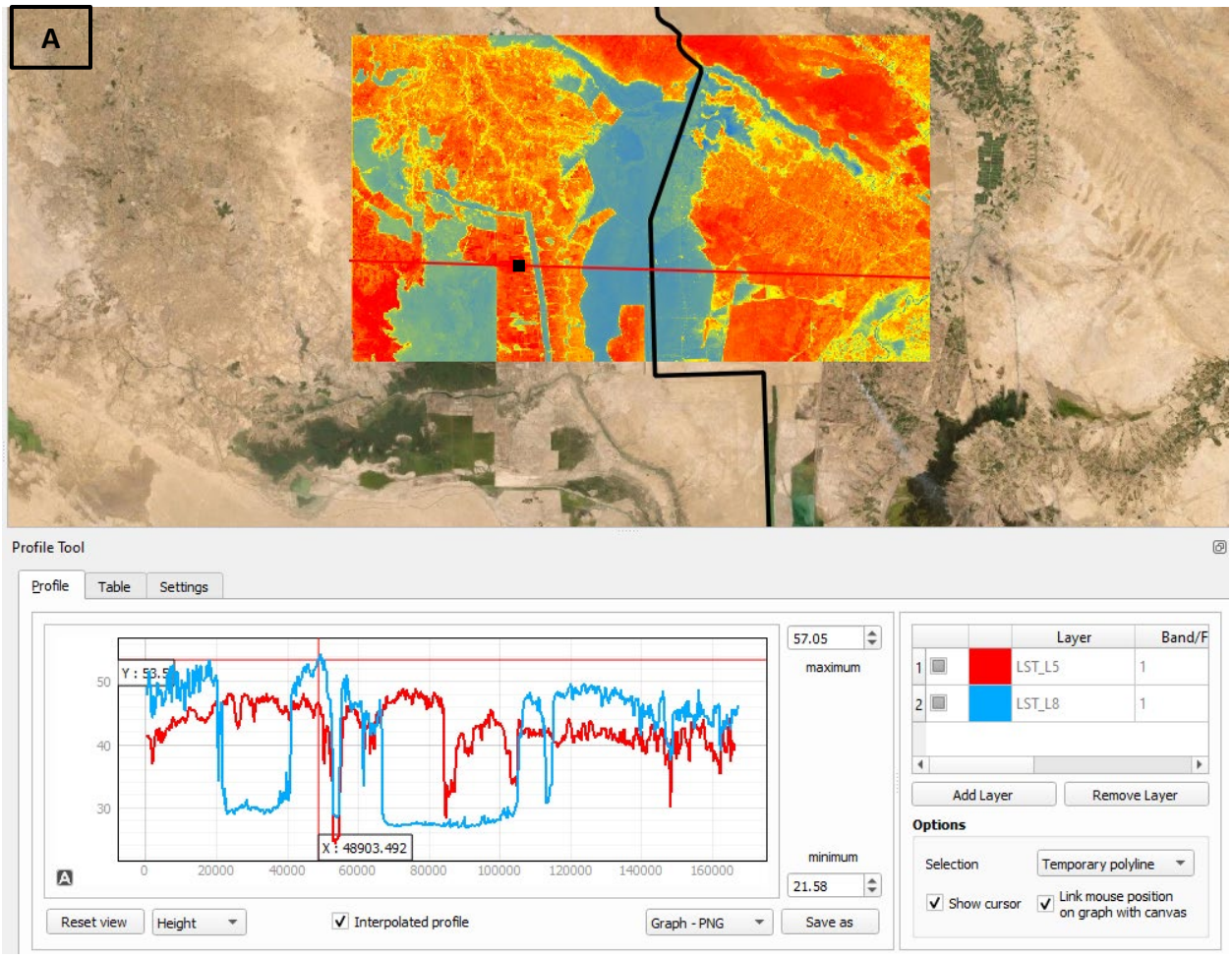

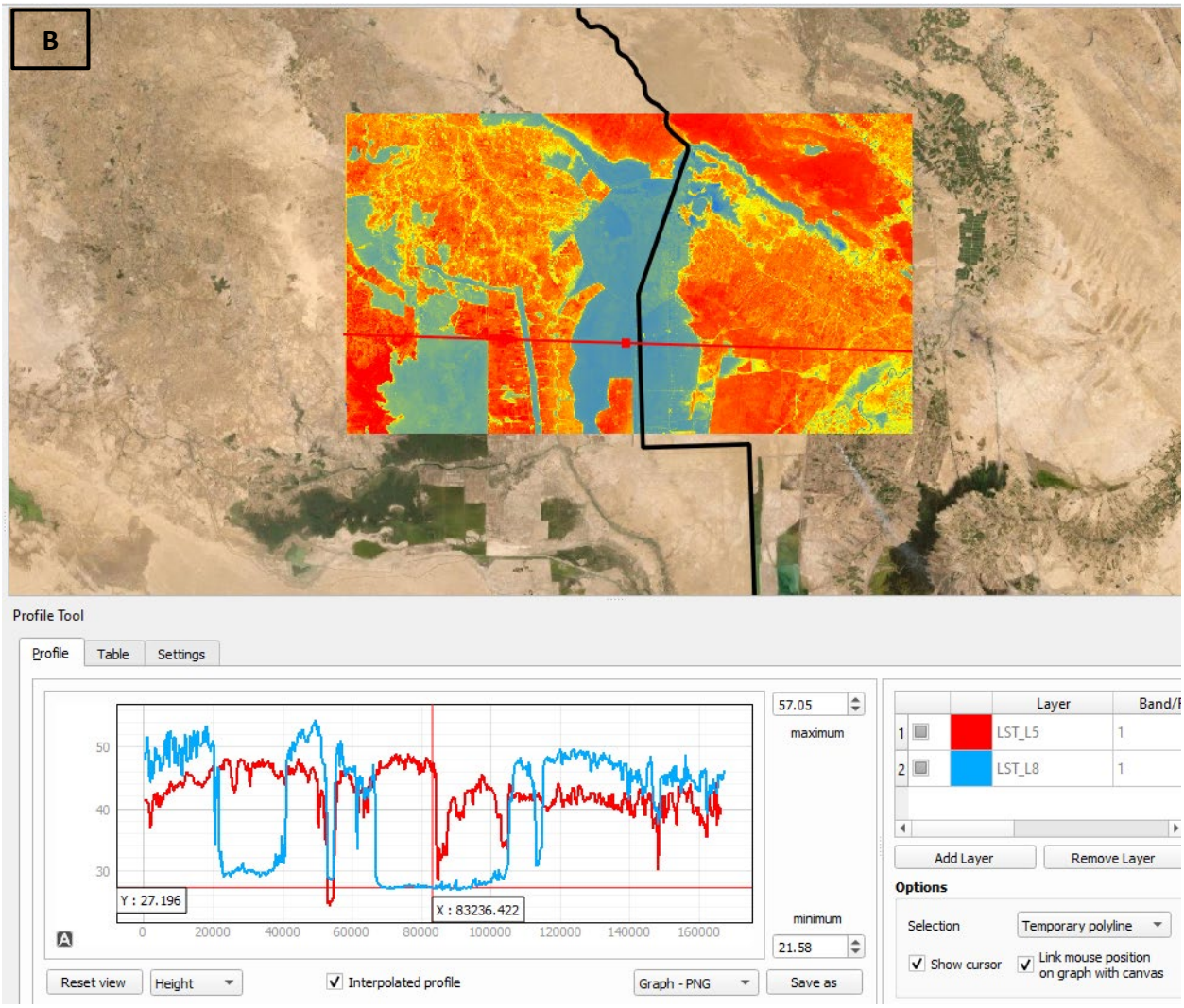
B
Profile Tool
Profile
Table
Settings
57.05
maximum
minimum
21.58
Y : 27.196
X : 83236.422
Layer
LST_L5
LST_L8
Add Layer
Remove Layer
Options
Selection
Temporary polyline
Show cursor
Link mouse position on graph with canvas
Reset view
Height
Interpolated profile
Graph - PNG
Save as

Appendix E

R Code ran in RStudio:

```
#######I. Random Forest Load Data#####
library(randomForest)
library(raster)
library(tidyverse)
library(readr)
install.packages("pdp")
library(pdp)
RF_Run <- read_csv("RF_Points.csv")
View(RF_Run)

########factors are only for categorical data and not continuous

###L8_Super
RF_Run$L8_Super<-as.factor(RF_Run$L8_Super)
is.factor(RF_Run$L8_Super)


###SpectralDi
RF_Run$SpectralDi<-as.factor(RF_Run$SpectralDi)
is.factor(RF_Run$SpectralDi)

###L5_Super
RF_Run$L5_Super<-as.factor(RF_Run$L5_Super)
is.factor(RF_Run$L5_Super)

###Summary
summary(RF_Run)

########Run Random Forest########
change.rf<-randomForest(SpectralDi~LST_L8+MNDWI_L8+SMMI_L8+SI_L8+
                          SMMI_L5+SI_L5+LST_L5+MNDWI_L5, data = RF_Run,
                        ntree = 4000, importance = T, proximity = T)
print(change.rf)
importance(change.rf)
varImpPlot(change.rf, main = "Variable Importance on al Hawizeh Marsh 2000 vs 2019")


###create ranked variable importance plots for each class
###values 0 = no change and 1 = change in wetland cover
###type 1 is to create the plot using mean decrease in accuracy

import0<-importance(change.rf, class="0", type=1)
```

```
import1<-importance(change.rf, class="1", type=1)

import0sort<-import0[order(import0[,1]),]
import1sort<-import1[order(import1[,1]),]

dotchart(import0sort, main="No Change", xlab = "Mean Decrease Accuracy")
dotchart(import1sort, main="Change",xlab = "Mean Decrease Accuracy")


################Partial Plot Function###################
###MDNWI_L8 AND each class change SUCH THAT 0 = no change and 1 = change
pdp.MNDWI_L8.plot1 <- partial(change.rf, pred.var="MNDWI_L8", prob=T, plot=T, which.class
= "1")
pdp.MNDWI_L8.plot1

pdp.MNDWI_L8.plot0 <- partial(change.rf, pred.var="MNDWI_L8", prob=T, plot=T, which.class
= "0")
pdp.MNDWI_L8.plot0

###LST_L8
pdp.LST_L8.plot1 <- partial(change.rf, pred.var="LST_L8", prob=T, plot=T, which.class = "1")
pdp.LST_L8.plot1

pdp.LST_L8.plot0 <- partial(change.rf, pred.var="LST_L8", prob=T, plot=T, which.class = "0")
pdp.LST_L8.plot0

###SMMI_L8
pdp.SMMI_L8.plot1 <- partial(change.rf, pred.var="SMMI_L8", prob=T, plot=T, which.class =
"1")
pdp.SMMI_L8.plot1

pdp.SMMI_L8.plot0 <- partial(change.rf, pred.var="SMMI_L8", prob=T, plot=T, which.class =
"0")
pdp.SMMI_L8.plot0
```

Appendix F

StoryMap link: https://storymaps.arcgis.com/stories/f8eac119c2db48aaa24ee1980054a1e3